Spring 5-11-2018

Targeted Triple Drug Regimen for the Treatment of Prostate Cancer

Tanuja Tummala
Pittsburg State University, ttummala@gus.pittstate.edu

TARGETED TRIPLE DRUG REGIMEN FOR THE TREATMENT OF PROSTATE CANCER

A thesis submitted to the Graduate School
in Partial Fulfillment of the Requirements
for the Degree of
Master of Science in Polymer Chemistry

Tanuja Tummala

Pittsburg State University

Pittsburg, Kansas

May 2018

TARGETED TRIPLE DRUG REGIMEN FOR THE TREATMENT OF PROSTATE CANCER

Tanuja Tummala

APPROVED:

Thesis Advisor _____
Dr. Santimukul Santra, Department of Chemistry

Committee Member _____
Dr. Dilip.K. Paul, Department of Chemistry

Committee Member _____
Dr. Irene Zegar, Department of Chemistry

Committee Member _____
Dr. Jian Hong, KPRC

ACKNOWLEDGMENTS

This thesis is the conclusion of my journey of master's which was just like climbing a high peak step by step, accompanied with encouragement, hardship, trust, and frustration. When I found myself at the top, experiencing the feeling of fulfillment, I realized though only my name appears on the cover of this dissertation, a great many people including my family members, well-wishers, my friends have contributed to accomplish this huge task.

A thesis becomes a reality with the kind of support and help of many individuals. I would like to extend my sincere thanks to all of them. First and foremost, I'm highly indebted to my supervisor, Dr. Santimukul Santra, who has supported me throughout my thesis with his patience and knowledge whilst allowing me the room to work in my own way. I attribute the level of my master's degree to his encouragement and effort, and without him this thesis, too, would not have been completed or written. One simply could not wish for a better or friendlier supervisor. It has been a period for intense learning not only in the scientific arena, but also on the personal level.

I would like to thank Dr. Peter Dvornic for providing me much greater support, guidance, all through my time in Pittsburg State University. I would like to thank Dr. Virginia Rider for letting me use her laboratory resources to complete my project. I thank Dr. Tuhina Banerjee to take out time to guide me to be on the correct path even though she was extraordinarily busy with her duties.

I would like to thank all my committee members Dr. Dilip K Paul, Dr. Irene Zegar, Dr. Jian Hong for generously offering their time, support, guidance and good will throughout the preparation and review of this document.

Further, I would like to thank all the faculty members for their valuable guidance which provided me with the tools that I needed to choose for going in right direction and to successfully complete my masters

My thanks and appreciation would go to all the friendly and cheerful group of my lab members and it is my radiant sentiment to place on record the deepest sense of gratitude to PSU, and I perceive this Master's program is the milestone in my career.

I would like to thank my family members for their wise counsel and sympathetic ear. You are always there for me.

TARGETED TRIPLE DRUG REGIMEN FOR THE TREATMENT OF PROSTATE CANCER

An Abstract of the Thesis by
Tanuja Tummala

Prostate cancer is the most common amongst men. According to ACS 2018 statistics, about 164,690 new cases appear and 29,430 deaths occur. Nearly 6 in 10 cases are diagnosed in men over 50 years of age and often there are no early symptoms. The treatment options include surgery, chemotherapy, hormonal therapy and/or radiation and it can often be treated successfully. However, the poor management and adverse effects demanded ways to find better treatment option. Towards the development of a personalized medicine for prostate cancer treatment, we proposed to design prostate cancer targeting magnetic nanoplatform. This integrates various key components such as combination of drugs, imaging agents, targeting ligands and targeted delivery of these cargos in high concentrations to tumor. A triple drug regimen of Oxaliplatin, Irinotecan and 5-Flurouracil was used, which was already known to be effective in the treatment of colorectal cancer and pancreatic cancer. These three drugs were encapsulated in folate conjugated magnetic nanoparticles and tremendous effect of cell death via oxidative stress in LNCaP cells was observed. The synthesis of magnetic nanoparticles, surface conjugation with folic acid using “Click” chemistry, encapsulations of cargos and their characterization were discussed in detail. Having folate conjugated magnetic nanomedicine, the drug delivery was targeted to prostate cancer and had no to minimal toxic effects on the healthy cells. Individual mechanism of the drugs and their synergistic effect in the treatment was evaluated by performing optical microscopy, magnetic resonance imaging experiments as well as cell-based assays such as ROS, apoptosis and necrosis, cytotoxicity, migration, and comet. This study showed us that the targeted nanoformulation which we designed was successful in exhibiting the toxic effects on a tumor cell.

TABLE OF CONTENTS

CHAPTER.....**PAGE**
I. INTRODUCTION.....1
1.1 Iron oxide nanoparticles.....2
1.2 Coating materials.....2
1.3 Targeting ligands.....4
1.4 Cancer statistics.....4
1.5 Nanotechnology in cancer.....5
1.6 Triple Drug Regimen..... 6
II. RESULTS AND DISCUSSION.....9
2.1.1 Synthesis and characterizations of iron oxide-based magnetic nanoparticles.....9
2.1.2 Stability studies.....13
2.1.3 Cytotoxicity assay.....13
2.1.4 Intracellular uptake studies of drug loaded IONPs.....14
2.1.5 Measure of ROS generation.....15
2.1.6 Quantification of apoptotic cell death.....16
2.1.7 Comet assay.....18
2.1.8 Migration assay.....20
2.2 Experimental section.....22
2.2.1 Materials.....22
2.2.2 Instrumentation.....22
2.2.3 Synthesis of PAA coated IONPs.....22
2.2.4 Encapsulation of DiI dye into IONPs.....23
2.2.5 Synthesis of propargylated IONPs.....23
2.2.6 Synthesis of azide functionalized folic acid.....23
2.2.7 Synthesis of folate conjugated IONPs.....24
2.2.8 Synthesis of drugs, dye encapsulating functional IONPs.....24
2.2.9 Cell Viability studies (MTT assay).....24
2.3.0 Cellular internalization by fluorescence microscopy.....25
2.3.1 Assessing the ROS generation.....25
2.3.2 Quantification of Apoptotic cell death.....26
2.3.3 Measure of DNA damage (Comet assay).....26
2.3.4 Detection of anti-metastatic potential (Migration assay).....26
III. CONCLUSION.....28
REFERENCES.....30

LIST OF TABLES

TABLE **PAGE**

Table 1 Cancer facts and figures- ACS 2018 statistics 5

LIST OF FIGURES

FIGURE **PAGE**

Figure1. Schematic representation of mechanism of action of drugs for prostate cancer treatment ..... ……6
Figure 2. DLS experiments of IONPs.....11
Figure 3. UV-Vis studies of IONPs, dye, drugs.....12
Figure 4. Stability studies……13
Figure 5. Cytotoxicity assay.....14
Figure 6. Cellular uptake studies 15
Figure 7. ROS generation in LNCaP cells 16
Figure 8. Apoptotic cell death in LNCaP cells.....17
Figure 9. Comet assay.....19
Figure 10. Quantitative analysis of comets……20
Figure 11. Migration assay..... …..21

LIST OF SCHEMES

SCHEME **PAGE**

Scheme 1. Synthesis of biocompatible iron oxide nanoparticles, surface functionalization and encapsulating anti-cancer drugs, optical dye within the pockets of iron oxide nanoparticles (IONPs)……....11

LIST OF ABBREVIATIONS

IONPs: Iron Oxide nanoparticles

PAA: Poly (acrylic acid)

IONP-COOH: Carboxylated iron oxide nanoparticles

IONP-FOL: Folate conjugated iron oxide nanoparticles

IONP-DiI-COOH: Carboxylated iron oxide nanoparticles carrying optical dye

IONP-DiI-FOL: Folate conjugated iron oxide nanoparticles carrying optical dye

IONP-drugs-DiI-FOL: Folate conjugated iron oxide nanoparticle carrying drugs and optical dye

ROS: Reactive oxygen species

DiI: 1, 1'-Dioctadecyl-3, 3, 3', 3'-Tetramethylindocarbocyanine Perchlorate

EDC/NHS: 1-ethyl-3-(3-dimethylaminopropyl) carbodiimide)

DAPI: 4', 6-diamidino-2-phenylindole

DLS: Dynamic light scattering

DMSO: Dimethyl sulfoxide

DHE: Dihydroethidium

FBS: Fetal bovine serum

MES: 2-(*N*-morpholino) ethane sulfonic acid

MTT: (3-(4, 5-dimethyl-thiazol-2-yl)-2, 5 diphenyl tetrazolium bromide)

NHS: N-hydroxy succinimide

PA: Propargyl amine

LNCaP cells: Lymph Node Carcinoma of Prostate Cancer cells

PBS: Phosphate buffer saline

LM Agarose: Low melting point agarose

IRI: Irinotecan

OXL: Oxaliplatin

5-FU: 5-Fluorouracil

LIST OF CHEMICAL STRUCTURES

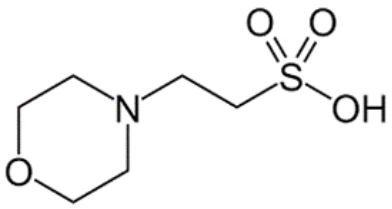

MES: 2-(N- morpholino) ethanesulfonic acid

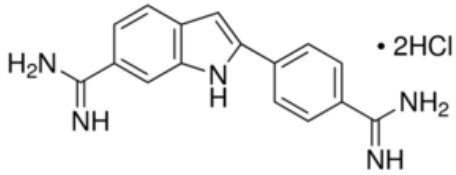

DAPI: 4', 6-diamidino-2-phenylindole

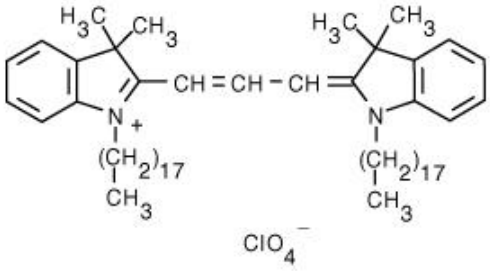

DiI

1, 1'-Dioctadecyl-3, 3, 3', 3'-Tetramethylindocarbocyanine Perchlorate

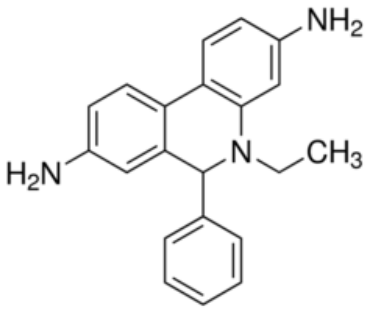

DHE

2, 7-Diamino-10-ethyl-9-phenyl-9, 10-dihydrophenanthridine, 3, 8 - Diamino-5, 6-dihydro-5-ethyl-6-phenylphenanthridine, Hydroethidine

MTT

(3-(4, 5-dimethyl-thiazol-2-yl)-2, 5 diphenyl tetrazolium bromide)

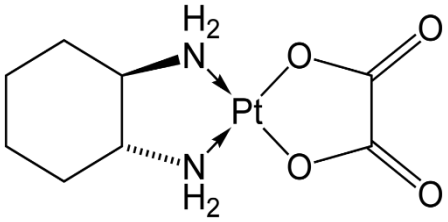

Oxaliplatin

[(1R, 2R)-cyclohexane-1, 2-diamine] 9ethanedioato-O, O') platinum (II)

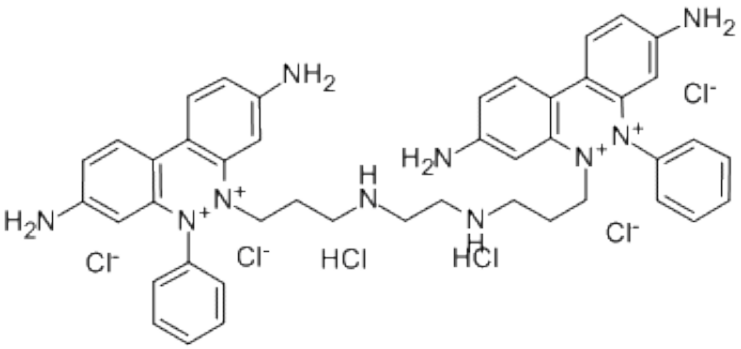

Ethidium homodimer

5, 5’ [ethylenebis (iminotrimethylene)] bis [3, 8-diamino-6-phenylphenanthridinium] dichloride

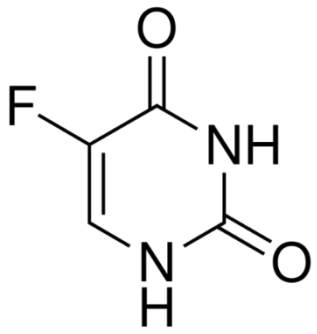

5-Fluorouracil

5-Fluoro-1H, 3H-pyrimidine-2, 4-Dione

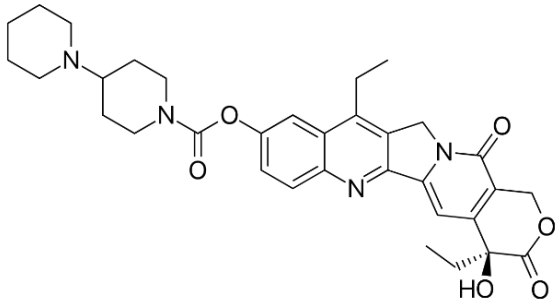

Irinotecan

(S)-4,11-diethyl-3,4,12,14-tetrahydro-4-hydroxy-3,14-dioxo 1H-pyrano[3’,4’:6,7]-indolizinol[1,2-b]quinoline-9-yl-[1,4’bipiperidine]-1’-carboxyate

CHAPTER I

IRON OXIDE NANOPARTICLES IN NANOMEDICINE FOR THE DIAGNOSIS AND TREATMNENT OF CANCER: A BRIEF OVERVIEW

1 INTRODUCTION:

Cancer is the most frightful disease in the world characterized by assemblage of many diseases. According to the American Cancer Society Cancer facts and figures 2018, it was reported that 87% of the cancer cases diagnosed in United States are in people of age 50 or older.[1] There are many known causes like smoking, unhealthy diet, lack of physical exercise, family history which may lead to the development of cancer. It was stated in a study by the American cancer society epidemiologists that 42% of the newly diagnosed cancer cases in 2018 are potentially avoidable.[1] Early detection and treatment, as well as a decline in smoking habits showed a drop of 26% of cancer cases for lung, colorectal, breast and prostate cancers from the years 1991-2015.[1] Cancer staging defines the degree of cancer at the time of diagnosis, which is essential for optimizing therapy and measuring prognosis. Several kinds of conventional treatment routes including chemotherapy, immunotherapy, hormone therapy, stem cell transplant, precision medicine, surgery, radiation therapy are available. The major draw backs of these conventional treatment approaches include harmful radiation use of hydrophobic anti-cancer drugs which have poor solubility, biocompatibility, and their effect on healthy cells finds difficulty in providing a better therapeutic effect.[2] Many studies are going all over the world to treat the cancer by minimizing the toxic effects to non-cancerous cells. In this respect, the nanomedicine plays a key role in enhancing the therapeutic efficacy of the anti-cancer drugs. The development of targeted drug delivery paved the path for cancer treatment with low toxicity to the healthy cells, targetability, improved bioavailability, specificity etc. Sechi et.al., conducted a study and the results presented that 43% people consider using nanotechnology for biomedical applications.[3]

There are many nanoplatforms for the cancer theranostics. Amongst all, iron oxide nanoparticles are used by many researchers because of their improved theranostic approach, magnetic properties, and biodegradability.

1.1 Iron oxide nanoparticles: Iron oxide nanoparticles fall under the category of magnetic nanoparticles, which are the chief class of nanoscale materials in current theranostics.[4] The capability of the iron oxide nanoparticles to work together at both cellular and molecular levels and their unique physical properties made perfect for use in several biomedical applications such as MRI contrast agents,[5] carriers for targeted drug delivery,[6,7] tissue repair, and immunoassay, detoxification of biological fluids, hyperthermia,[8] and in bio-separation, biosensors.[9-14] There are many synthetic protocols for iron oxide nanoparticles like the co-precipitation method,[15] thermal decomposition method, [16] hydrothermal method,[17] microemulsion method,[18] Sonochemical method,[19] and microwave assisted synthesis[20] with their own merits and demerits which were previously reported.[21] The average hydrodynamic diameter of these nanoparticles needs to be less than 100 nm to achieve targeted drug delivery and any other biomedical applications. On the other hand, there should also be a special surface coating which needs to be non-toxic and biocompatible and allows targeted drug delivery with a specific localization in the area. It was stated in a study that hydrophobic iron oxide nanoparticles, when entered the blood stream, are fenced by the hydrophobic plasma proteins through a process called as opsonization.[22] After entering the physiological environment, there will be formation of a clump due to the contacts of hydrophobic-hydrophilic surfaces. This tends to clear the hydrophobic iron oxide nanoparticles through the process of mononuclear phagocytic system. In order to avoid this fast clearance from the system and to increase the stability, in vivo circulation, and functionality there is a need of hydrophilic coating on the surface of iron oxide nanoparticles. This makes the iron oxide nanoparticles a multifunctional theranostic agent by serving the purpose of both diagnosis and targeted therapy.

1.2 Coating materials: There are several studies which used different kinds of coating materials on the surface of iron oxide nanoparticles. A) Chitosan, a natural polymer obtained from sea sources which is bio-compatible, hydrophilic, bio-degradable, non-antigenic and non-toxic coating on the iron oxide nanoparticles (IONPs) surface has shown that it was used to provide better contrast

agent for MR imaging and in therapeutic gene delivery.[23-30] B) Polyethylene Glycol (PEG), a water soluble polymer which is reported to increase the aqueous solubility of hydrophobic drugs [31-34] and increases the circulation time by minimizing the uptake by the mononuclear phagocytic system. [35,36] It was also reported that PEG acts as a good spacer for the attachment of different biomolecules.[37-42] C) Dextran, a polysaccharide which is known to be widely used in many biomedical applications, like MR imaging and commercially available contrast agents, and has been shown to process cancer nodal staging capabilities.[43] Introducing a carboxy methyl group to the dextran coating improves the stability and functionality. A study was conducted on Porcine aortic endothelial cells in both 2D and 3D cell culture tests in which the cells were treated with 5 nm and 30 nm diameter IONPs coated with Dextran or PEG. The results showed that the cell viability was deceased upon treating with undecorated nanoparticles, whereas there was no reduction in cell viability when treated with Dextran and PEG coated IONPs. It was also stated that the undecorated nanoparticles induced significant formation of reactive oxidative species (ROS) and the IONPs coated with dextran or PEG did not increase the ROS levels. On the other hand, dextran and PEG coatings decreased the fluorescence intensity by 35.2% and 62.6% respectively.[44] D) Poly (vinyl alcohol) which is a water soluble synthetic polymer has been successfully utilized for the drug delivery and other biomedical applications like tendon repair, ophthalmic materials, contact lenses etc. Because of having the properties of resisting protein adsorption and cell adhesion and high biocompatibility, it was reported to be used as an excellent coating material on the surface of IONPs. Different percentages of PVA coating on the IONPs surface using the anti-cancer drug Doxorubicin for drug delivery was studied by Kayal et.al.[45] It was concluded that carboxy-PVA coating had excellent thermal stability and the amino-PVA had higher cellular uptake because of the negative charge of carboxylic acids and positive charge of amine groups respectively. E) Poly (vinyl pyrrolidone), a water-soluble polymer having neutral charge, aqueous solubility and biocompatibility has been coated on the surface of IONPs for use in different biomedical applications. The results from many studies showed there is an increase in the stability of IONPs in physiological media.[46] It was stated that the PVP coated IONPs will be very encouraging for clinical applications because of their monodispersity and solubility. F) Poly (acrylic acid), synthetic high molecular weight polymer of acrylic acid is known to enhance the biocompatibility, stability of the nanoparticles and

facilitates the bioadhesion.[47] G) Poly (Lactic-co-glycolic acid), PLGA, a co-polymer with biocompatibility and biodegradability, approved by Food and Drug Administration was used as a coating on the surface of iron oxide nanoparticles.[48-50]

1.3 Targeting ligands: Using the different nanoparticle systems for biomedical applications, there is a need of targeting ligands or specific proteins in derivatizing the IONPs. A) Transferrin, which is an iron-binding blood plasma glycoprotein, regulates the level of free iron in biological fluids. It is extensively used as a targeting ligand in the active pointing of anti-cancer agents, proteins, genes to mainly multiplying cells through transferrin receptors.[51-54] B) TAT peptide derived from the Trans-activator of transcription (TAT) of human immunodeficiency virus is a cell membrane-penetrating peptide which enhances the intracellular delivery.[55,56] C) Folic acid, a water soluble B9 vitamin obtained from many sources like green leafy vegetables, liver, yeast etc. is used in treating megaloblastic anemia. In cancer therapy, folic acid acts as a common targeting ligand because of its poor immunogenic property and facilitates the internalization of particles due to the over expression of folate receptors on the cancerous cells.[57]

1.4 Cancer statistics: According to the American Cancer Society, there are many estimated new cases and deaths in 2018 due to different types of cancer which is mentioned below in the tabular form, table 1. It was seen in the results that there were more number of new cases for prostate cancer compared to other cancer types, so nanoformulation was designed targeting the prostate cancer. The most common type of cancer among men is the prostate cancer. The risk of prostate cancer is about 6 in 10 men of age 65 or older are diagnosed with prostate cancer. According to the American cancer statistics, it was said that the average age of a person to be diagnosed with prostate cancer is about 66 and very few people were diagnosed before the age of 40. After lung cancer, prostate cancer is the second leading cause of death in men.[58]

Sites of cancer	Estimated new cases in 2018	Estimated deaths in 2018
Prostate	164,690	29,430
Lung & Bronchus	121,680	83,550
Colon & Rectum	75,610	27,390
Urinary bladder	62,380	12,520
Kidney & Renal pelvis	42,680	10,010
Liver & Intrahepatic bile duct	30,610	20,540
Non-Hodgkin Lymphoma	41,730	11,510
Leukemia	35,030	14,270

Table 1: Leading sites of new cancer cases and deaths- American Cancer Society facts and Figures 2018 Estimates.

1.5 Nanotechnology in cancer: A wide variety of nanotechnology-based approaches are available for the diagnosis and drug delivery. Different nanoplatforms including iron oxide nanoparticles (IONPs), gold nanoparticles (AuNPs), cerium oxide nanoparticles or nanoceria (CeONPs/NC), polymeric nanoparticles (PNPs), carbon nanotubes (CNTs) and quantum dots (QDs) play a vital role in biomedical applications.[59-64] In addition, iron oxide nanoparticles have dual modalities of both MR detection and targeted drug delivery when conjugated with receptor targeting molecules or antibodies. These features prompted us to formulate magnetic nanomedicine (MnM) containing three drugs combination including irinotecan, oxaliplatin, and 5-fluorouracil to combat prostate cancer (**Figure 1**)

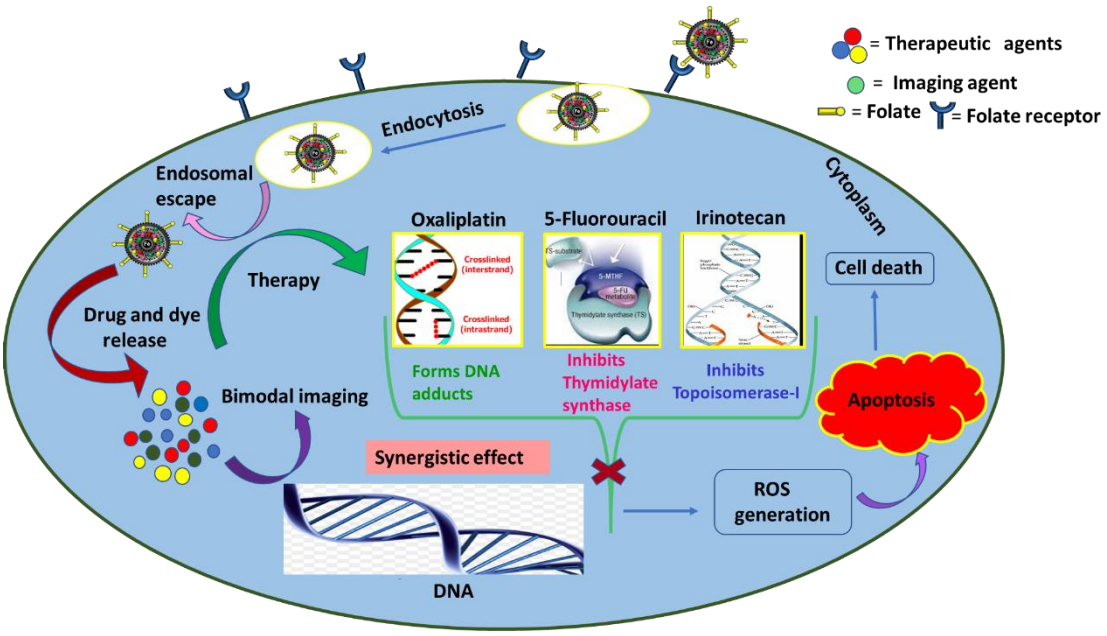

.

Figure 1. Schematic representation of mechanism of action of combination of three drugs for prostate cancer treatment.

1.6 Triple Drug Regimen : Many studies have shown that the combination of three drug regimen of irinotecan, 5-Fluorouracil, oxaliplatin was well known to be effective in treating metastatic colorectal cancer[65] and pancreatic cancer.[66] The synergistic or additive interaction between SN-38 (active metabolite of irinotecan) with oxaliplatin and 5-FU was reported in several studies.[67-70] Having the dose limiting toxic effects and different mechanism of actions, the combination of irinotecan and 5-FU, oxaliplatin and 5-FU, irinotecan and oxaliplatin have been broadly used in the clinical trials.[71] Several phase III studies indicated that the combinations of irinotecan and 5-FU/Leucovorin (FOLFIRI), oxaliplatin and 5-FU/Leucovorin (FOLFOX) have an increased therapeutic efficacy and antitumor activity when compared with 5-FU/Leucovorin alone.[72-75] The results from phase III studies revealed that irinotecan when combined with 5-FU/LV has sustained the survival rates compared to 5-FU/LV alone.[76] Also, it is reported that oxaliplatin in combination with 5-FU/LV as a first line chemotherapeutic regimen in a small group of unresectable metastatic colorectal cancer patients showed 30-40% survival without evidence of disease for more than 5 years.[77,78] A randomized study on untreated metastatic

colorectal cancer patients indicated that patients were treated with FOLFIRI [irinotecan, leucovorin, and 5-FU] followed by FOLFOX-6 [oxaliplatin, leucovorin, and 5-FU] on arm A and the reverse on arm B. The results from this study revealed there are similar therapeutic efficacies and the survival rates were 21.5 months and 20.6 months for arm A and arm B, respectively. These suggests that the treatment of metastatic colorectal cancer patients with these three drugs is associated with promising survival.[79] In another report, the FOLFOX-4 regimen [oxaliplatin, folinic acid, 5-Fluorouracil] had higher survival rates compared to IFL [irinotecan, 5-Fluorouracil, leucovorin], as only 24% patients on IFL were able to take oxaliplatin as a second line treatment, whereas 60% of the patients were able to receive irinotecan as the second line treatment on FOLFOX-4.[80] To develop a new chemotherapy regimen with more therapeutic efficacy, the combination of irinotecan, oxaliplatin,5-fluorouracil was used as first line treatment in 42 metastatic colorectal cancer patients and the results of phase I-II studies showed there is 71.4% overall response rate, median progression free survival of 10.4 months and median overall survival rates of 26.5 months.[81] The first line treatment of 31 metastatic colorectal cancer patients with irinotecan, oxaliplatin,5-fluorouracil achieved 58% overall response rate and adverse effects of neutropenia in 45% patients, 3-4 grade diarrhea in 32% patients.[82] In a study, patients with advanced solid tumors given increasing doses of irinotecan, oxaliplatin followed by simplified LV/5-FU showed 78% grade 3-4 neutropenia and 27% grade 3-4 diarrhea.[83] Another study showed that 26 patients treated with irinotecan, oxaliplatin, 5-FU and leucovorin had adverse effects of 38% patients with grade 3-4 neutropenia and 34% patients with grade 3-4 diarrhea.[84] Many other studies reported the feasibility of this triple drug combination.[85-87] It was indicated by several studies that the best results were attained in patients treated with all the three active agents (irinotecan, oxaliplatin, 5-fluorouracil) and synergistic effect was achieved by using in the order of irinotecan-oxaliplatin-5-fluorouracil.[88] Phase III trials revealed higher survival rates, progression free-survival when irinotecan was administered along with the combination of 5-FU/leucovorin in comparison to 5-FU based regimens.[72,73] A study with oxaliplatin stated that there is high response rate, time to tumor progression and survival rate when oxaliplatin is combined with 5-FU/LV.[89] It was stated by a trial that infusional 5-FU regimens show low response rates compared to combination of infusional and bolus administration of 5-FU/LV alone.[75,90] A study stated that adding oxaliplatin to 5-FU/Leucovorin progresses the outcome of patients with colorectal

cancer.[89] Trials were carried out on using oxaliplatin and 5-FU in combination[91,92] and compared with administration of oxaliplatin alone[74] and 5-FU alone.[75,90] A study was performed on the therapeutic activity of irinotecan in colorectal cancer patients which showed there is a noteworthy effect of irinotecan.[72,73,75,93-96] Irinotecan when used as a first line drug showed more therapeutic efficacy as 5-FU/LV.[73] In a randomized study, irinotecan was combined with 5-FU/LV and the results were compared with 5-FU/LV alone. These studies reported longer time to progression, greater response rate in the combination therapy.[72,73] The growth inhibitory effect was observed when oxaliplatin was administered after irinotecan.[69] They also conducted a trial on sequential administration of irinotecan prior to 5-FU and observed a synergistic effect.[67] Preclinical trials were performed on two drug combinations of oxaliplatin and irinotecan[69], irinotecan, and 5-FU[67,97],oxaliplatin and 5-FU.[98,99] Phase II studies with the combination of 5-FU/LV with oxaliplatin showed that this combination prolonged the progression free survival.[90,100-102]

Conclusion: In conclusion, based on above-mentioned results from pre-clinical trials and clinical trials, it was proven that the three anti-cancer agents (irinotecan, oxaliplatin, 5-fluorouracil, **Figure 1**) were effective in treating metastatic colorectal and pancreatic cancers.[65,66] But due to the lack of targeted delivery, there are many side effects to the non-cancerous cells. To overcome this, a nanoformulation which can deliver drugs to the targeted sites was developed. As prostate cancer is the second leading cause of death in men,[58] the synthesized nanoparticles were treated on human prostate cancer cell lines to check the similar therapeutic efficacy of the combination of three drugs (irinotecan, oxaliplatin, 5-fluorouracil). The results from our studies showed that the nanoformulation has minimal side effects on healthy cells and was very effective in treating prostate cancer.

CHAPTER II

2.1 RESULTS AND DISCUSSION:

2.1.1 Synthesis and characterization of IONPs: Polyacrylic acid-coated superparamagnetic iron oxide nanoparticles were synthesized using a water-based precipitation method as shown in **[** 4.0 × 10^{-3} M **(1, Scheme 1)]** as reported previously.[103] The iron oxide nanoparticles are known in biomedical applications like targeted drug delivery, immunoassay, detoxification of biological fluids, MRI tracker, treating hyperthermia, tissue repair, bio-separation and biosensors[5-14.] The synthesized IONPs were centrifuged to remove the bigger size IONPs. To get rid of the unreacted drugs and dye molecules, the resulting IONPs were purified using the dialysis method in a dialysis bag having molecular weight cut off range (MWCO of 6-8 kDa) as previously reported by Santra et, al.[104] In order to use the IONPs for biomedical applications, an average size of below 100 nm is very important. So, we characterized the IONPs for average size and surface charge (zeta potential) using Zetasizer ZS90. The average size of the IONP-COOH was 41 ± 3 nm **(Figure 2A)** and the zeta potential was -24.3 mV **(Figure 2B)**. For the addition of optical modality, 2.0 µL of 5 µM fluorescent dye DiI was encapsulated in the IONP-COOH **[**2ml, 3.4 × 10^{-3} M **(2, Scheme 1)]**. The IONP-COOH was propargylated and pegylated in which the pegylation plays the role in enhancing the aqueous solubility of the drugs and also it was reported that PEG acts as a good spacer for the attachment of different biomolecules[37-42] and the propargylation **[**2 ml, 3.0 × 10^{-3} M **(3, Scheme 1)]** facilitates in performing “Click” chemistry by reacting with azide functionalized folic acid in presence of CuI as a catalyst **[**2 ml, 2.2 × 10^{-3} M **(4, Scheme 1)],** as reported earlier.[105] The folate functionalized IONPs plays a major role in targetability to the tumor. After successful conjugation of the targeting ligand, folic acid on the surface of IONP, they were characterized for hydrodynamic diameter and surface zeta potential. The average size of the folate functionalized IONP was found to be 46 ± 2 nm **(Figure 2C)** and the zeta potential was found to be -22.6 mV

(Figure 2D). To provide optical modality and therapeutic efficacy, the folate functionalized IONPs were encapsulated with 2.0 µL of 5 µM DiI dye **[**2.2 × 10 $^{-3}$ M **(2, Scheme 1)]** and 5.0 µL of 2.0 mM irinotecan, 5.0 µL of 2.0 mM 5-Fluorouracil and 5.0 µL of 2.0 mM oxaliplatin **[**2.0 × 10 $^{-3}$ M **(5-8, Scheme 1)]** using the solvent diffusion method.[106] To get rid of the unreacted drugs and dye molecules, the folate functionalized IONPs carrying the therapeutic drugs and optical dye (IONP-DiI-drugs-FOL) was dialyzed for 2 h against DI water by periodical water change. The dialyzed IONP-drugs-DiI-FOL was incubated on table mixer for 2 h at room temperature. It was labelled and

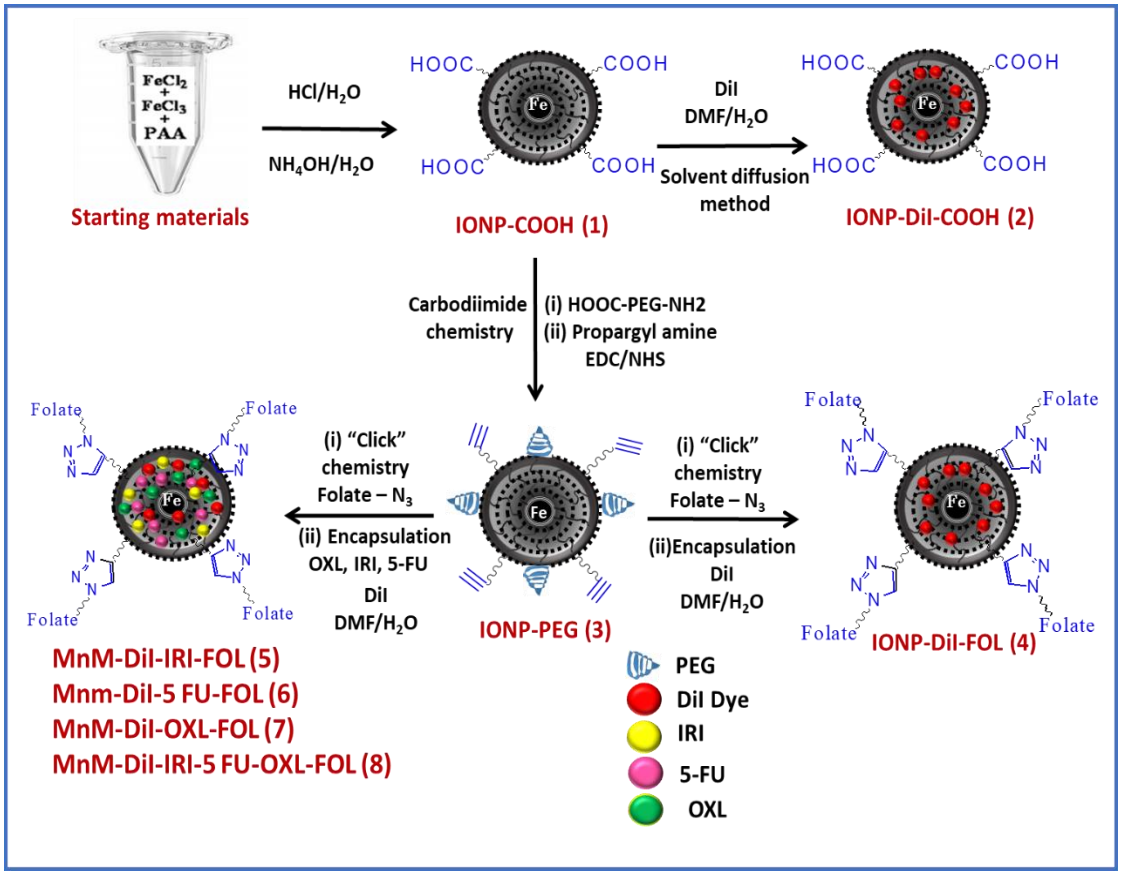

stored at room temperature for further characterizations. The IONPs carrying drugs and dye **(5-8, Scheme 1)** was characterized for average size and zeta potential. The results were found to be 48 ± 2 nm **(Figure 2E)** and -23.1 mV **(Figure 2F)**.

Scheme 1: Synthesis of biocompatible IONP-COOH **(1)** and encapsulated fluorescent dye using solvent diffusion method **(2)**. Using EDC-NHS chemistry, the IONP-COOH was propargylated and pegylated **(3)**. Using "Click" chemistry, IONP surface was conjugated with folic acid **(4)**.

Therapeutic drugs irinotecan, 5-Fluorouracil, oxaliplatin and fluorescent dye DiI were encapsulated into the folate nanoparticles to formulate a personalized nanomedicine for the treatment of prostate cancer **(5-8)**.

To check the successful encapsulation of the drugs and dye and the conjugation of the surface functionality, the UV-Vis and fluorescence spectrophotometric analysis was performed using a Tecan i-control plate reader. The specific absorbance and fluorescence bands **(Figures 3A** & **3B)** indicated the presence of folic acid . The absorption spectrum of FOL, DiI dye at wavelengths of 335 nm, 587 nm, respectively, was shown in **Figure 3C**. In **Figure 3D**, the presence of DiI dye at a fluorescence emission of 585 nm was observed. **Figure 3E** shows the presence of FOL, IRI at UV-Vis absorption wavelengths of 335 nm, 635 nm, and **Figure 3F** indicates the presence of IRI at a fluorescence emission at the wavelength of 680 nm.

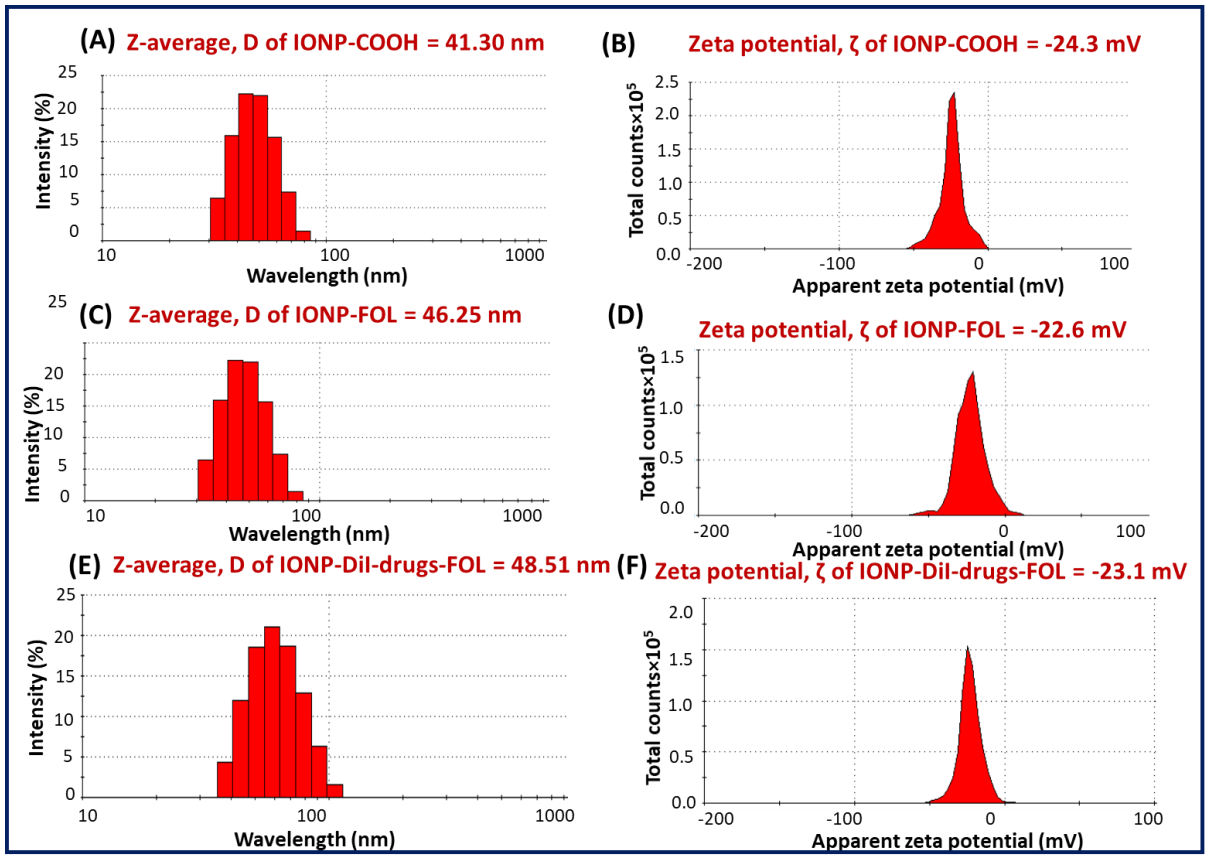

Figure 2: Dynamic light scattering experiments represents IONP-COOH, IONP-FOL and IONP-DiI-drugs-FOL with an average hydrodynamic diameter of 41 ± 3 nm , 46 ± 2 nm, and 48 ± 2 nm, respectively, and the zeta potential of IONP-COOH , IONP-FOL and IONP-DiI-drugs-FOL are -24.3 mV , -22.6 mV, and -23.1 mV respectively.

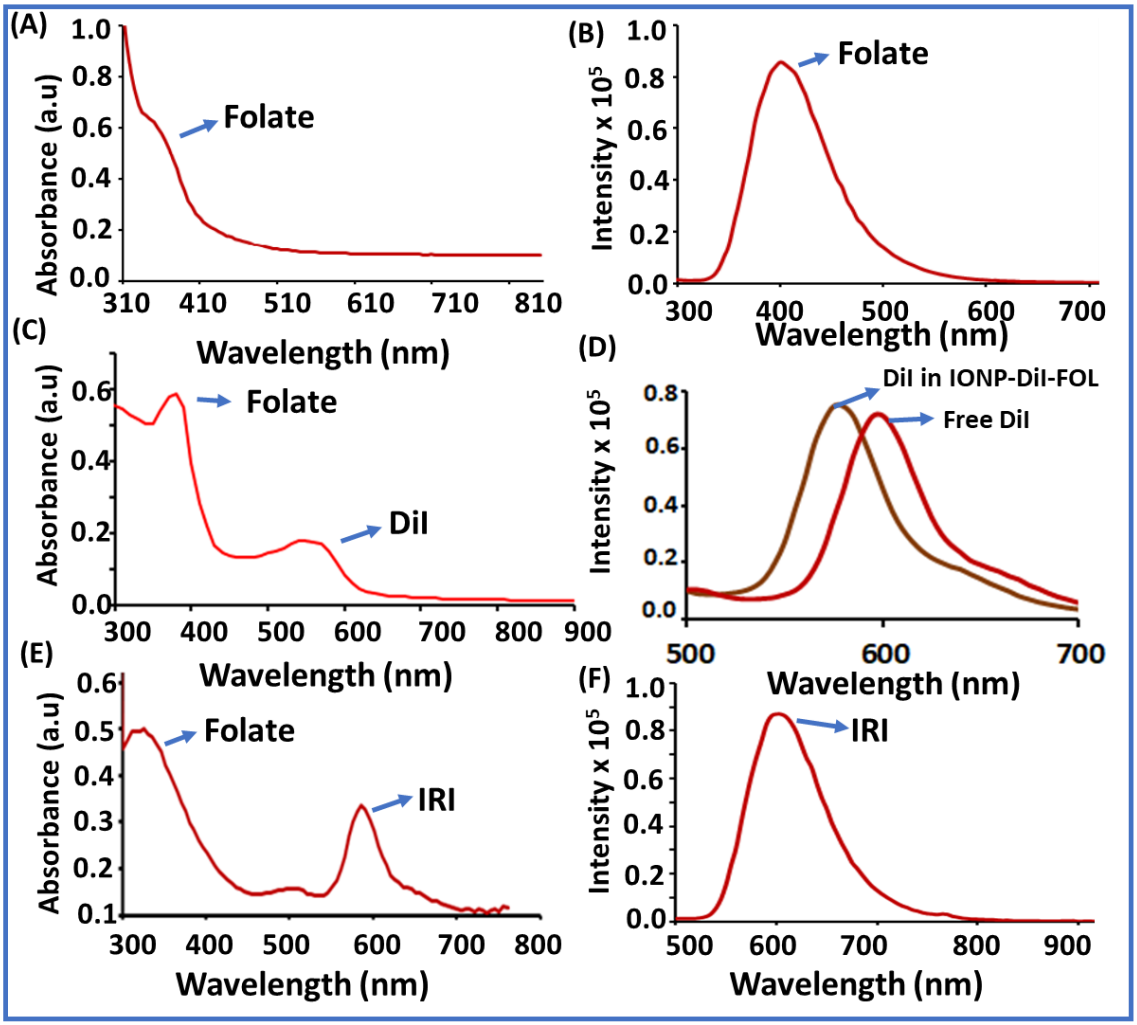

Figure 3: (**A**) UV-Visible absorption (λ_{abs}= 335 nm) and (**B**) Fluorescence emission spectra (λ_{max}= 450 nm) indicates the presence of folic acid in IONP-FOL. (**C**) UV-Visible absorption spectrum with bands at 335 nm, 587 nm shows the presence of folic acid, DiI dye respectively in IONP-DiI-FOL. (**D**) Fluorescence emission spectrum showing band at 585 nm indicates the presence of DiI dye in IONP-DiI-COOH. (**E**) UV-Visible absorption spectrum with bands at 335 nm, 635 nm indicates the presence of folic acid, irinotecan respectively in IONP-DiI-drugs-FOL. (**F**)

Fluorescence emission spectrum with band at 680 nm indicates the presence of irinotecan in IONP-DiI-drugs-FOL.

The results from DLS showed that the iron oxide nanoparticles synthesized were having smaller size and the negative zeta potential which are ideal for the biomedical applications. In addition to that, the UV-Vis and fluorescence studies indicated the successful conjugation of the surface groups and encapsulation of drugs , fluorescent dye.

2.1.2 Stability studies: Before treating the cells with the nanoparticles, the stability of the nanoparticles in different media including 1X PBS (pH = 7.4) and 10 % FBS was checked by measuring the average size of the nanoparticles at different time periods on 1 day, 7 days, 30 days, and 60 days. The results showed there was no much change in the size of the nanoparticles which indicates that the nanoparticles were stable with time.

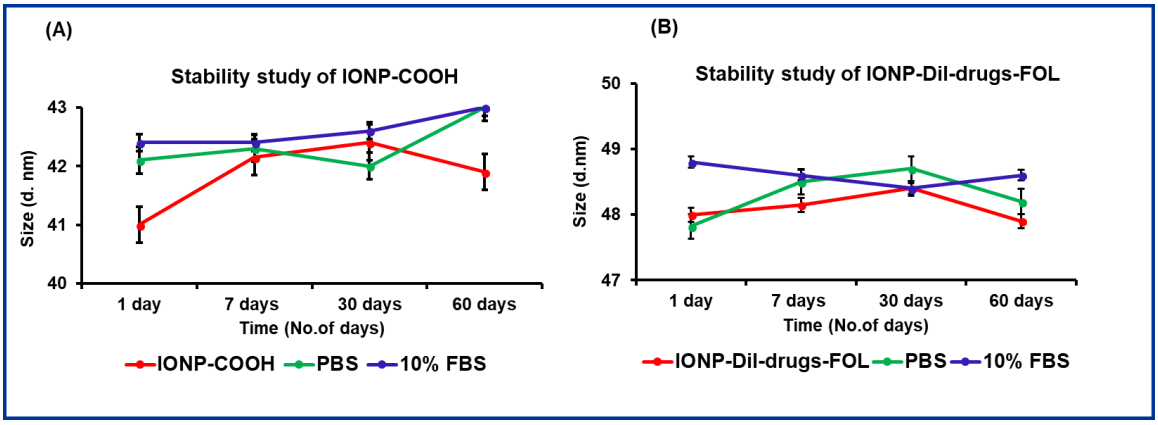

Figure 4: Determination of stability of the nanoparticles in different media including 1X PBS (pH = 7.4) and 10 % FBS at different time points. Figure 4 (A) shows the stability of IONP-COOH and Figure (B) shows the stability of IONP-DiI-drugs-FOL.

The results indicated that the nanoparticles are very stable with time

2.1.3 In-vitro Cell viability (MTT assay): To know the therapeutic efficacy and cytotoxicity of the nanoparticles carrying our therapeutic drugs, concentration dependent cell viability assay or MTT assay was performed. The theory behind MTT assay is when the yellow colored MTT is added

to the cells treated with nanoparticles, a purple color formazan was formed. The intensity of the formazan formed is directly proportional to the amount of number of live cells. To perform MTT assay, both the cell lines Lymph node Carcinoma of Prostate Cancer (LNCaP) and PC3 cells were cultured and seeded in a 96 well plate on the previous day of experiment. The cells were incubated for 24 h at 37 ℃ in the presence of 5% CO_2. On the day of experiment, the cells were treated with nanoparticles carrying the drugs individually and in combination (irinotecan+5-FU+oxaliplatin). After 24 h of incubation, MTT solution (30 µL , 5 mg/ml) was added in each well and incubated for 4-6 hrs. The formazan crystal formed were dissolved using acidic solution (75 µL , 10 mL isopropanol + 250 µL HCl) and the absorbance of the formazan formed was read using Tecan i-control Plate reader. Very promising results were observed. There was about 85% of cell death in LNCaP cells **(Figure 5A)** within 24 h and very less cytotoxicity was seen in the PC3 cells **(Figure 5B)** on treatment with different doses of the drugs individually and in combination. This experiment indicated that nanoparticles can deliver therapeutic drugs only to the cancer sites, when targeted.

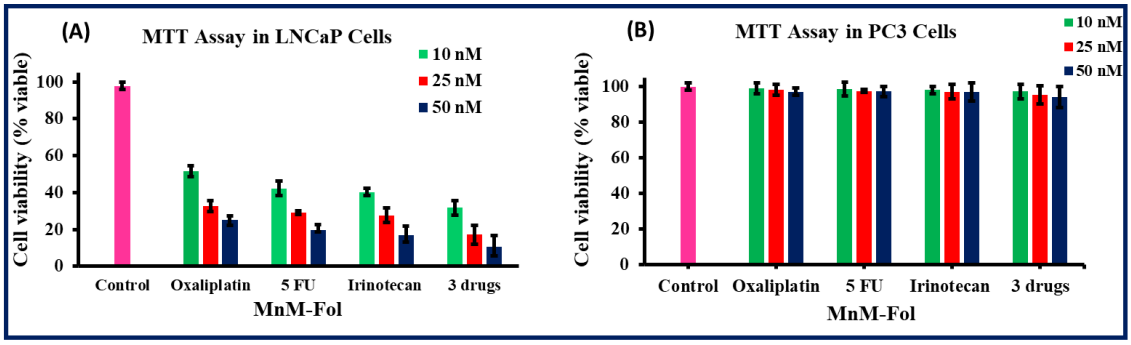

Figure 5: Determination of cytotoxicity within 24 h of incubation in LNCaP (**A**) and PC3 cells (**B**) using MTT assay. **A**) It shows the concentration dependent cell death upon treatment with the drugs individually and in combination. **B**) Minimal or no toxicity was observed in PC3 cells when treated with nanoparticles carrying individual drugs and in combination.

The results from MTT assay revealed the cell death upon the treatment of the LNCaP cells with nanoparticles and there is minimal toxicity in the control cell line, PC3 cells.

2.1.4 Intracellular uptake of cargos loaded IONPs: After observing the cytotoxicity of our nanoparticles carrying drugs on LNCaP cells, we were interested in visualizing the cell death. For that, cellular uptake studies were carried out on LNCaP cells and PC3 cells using nanoparticles with different functionalities. The cells were grown in petri dishes by supplying nutrient media and treated with nanoparticles. The cells were fixed using 4% paraformaldehyde and stained the nucleus with DAPI. The fluorescence microscopic images were obtained using IX73 Olympus microscope. The results showed non-internalization upon treating LNCaP with IONP-DiI-COOH **Figures 6A-6D**). The internalization of the nanoparticles was observed when the cells were treated with folate functionalized IONP carrying DiI dye. **(Figures 6E-6H**), and the cell death was noticed when the cells were treated with IONP-DiI-drugs-FOL **(Figures 6I-6L)**. Also, PC3 cells were seeded as a control cell line and it was observed that folate nanoparticles were not internalized into PC3 cells due to the lack of folate receptors. (**Figures 6M-6P**)

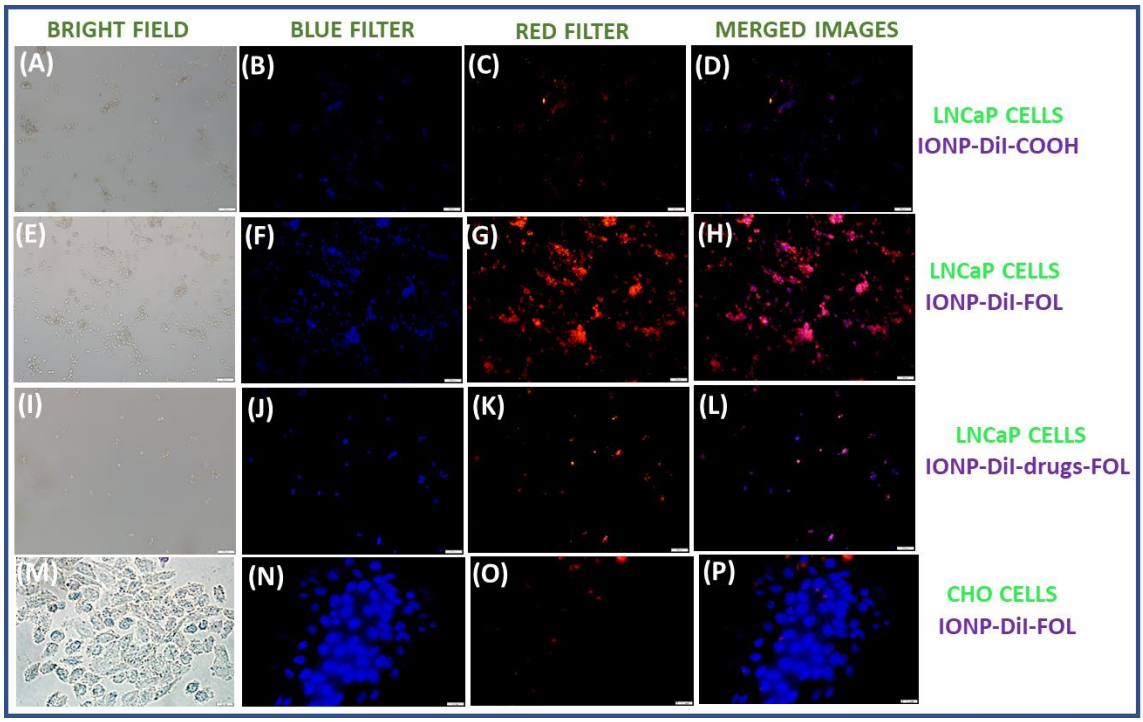

Figure 6: Fluorescence microscopic images in bright field and corresponding blue filter, red filter, and merged images. (**A-D**) showing non-internalization, (**E-H**) showing internalization, (**I-L**) showing cell death in LNCaP cells and (**M-P**) showing non-internalization in PC3 cells.

2.1.5 ROS generation in LNCaP cells: The results from cellular uptake studies made us to explore the literature for understanding the possible reason behind cell death. For this, we performed an in vitro assay known as ROS. ROS plays a major role in cell signaling pathway and hemostasis. In this experiment, a fluorescent dye named Dihydroethidium (DHE) was used. In theory, DNA dye DHE which is usually blue in color by itself is oxidized to 2-hydroxyethidium in presence of ROS generation. The 2-hydroxyethidium gives red fluorescence. For this study, the LNCaP cells were seeded in 12-well plates and grown for 24 h. When the cells were 80-90% confluent, the nanoparticles were added and incubated for different time points at 6 h, 12 h, 24 h respectively. The cells were washed, stained with 32mM DHE dye and the fluorescence microscopic images of the cells were captured using an Olympus IX73 microscope. **Figures 7A & 7B** showed the levels of ROS generation in cells at 6 h, **Figures 7C & 7D** at 12 h, and **Figures 7E & 7F** at 24 h of nanoparticle treatment in the bright field, and its corresponding red filter respectively.

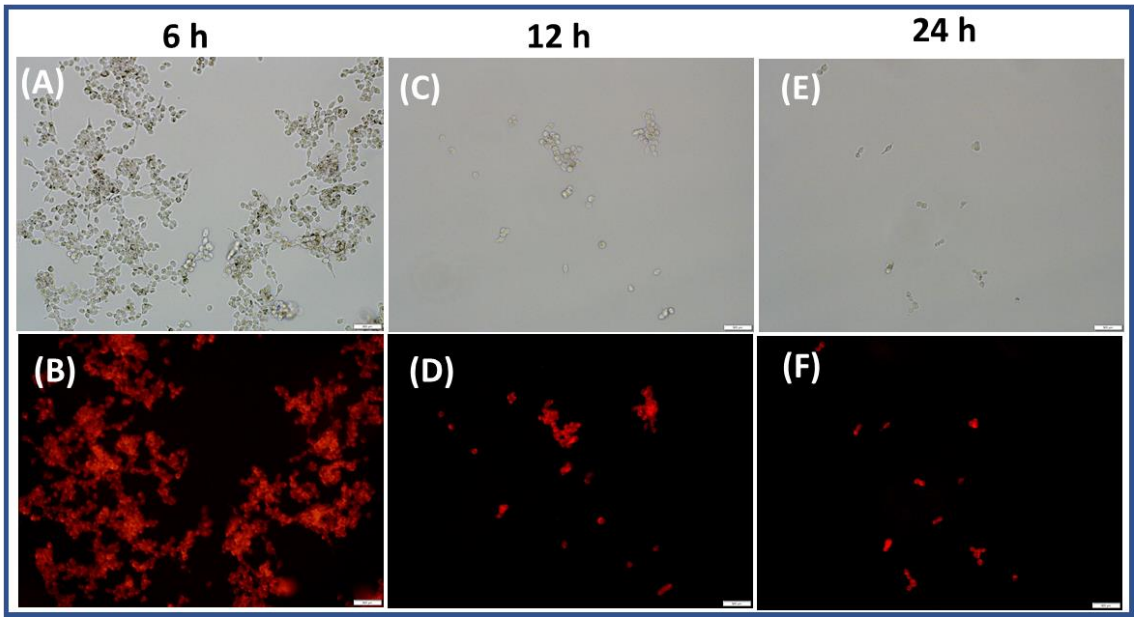

Figure 7: Measure of ROS generation in LNCaP cells at different time points 6h, 12h, and 24 h in bright field and corresponding red filter.

2.1.6 Apoptotic cell death in LNCaP cells: The generation of ROS eventually leads to apoptosis. Apoptosis is nothing but the programmed cell death in which the protrusion of plasma membrane occurs. This can be initiated by either intrinsic or extrinsic pathways. Here, the intrinsic pathway applies as the cells kills itself by sensing the stress. The basic principle behind apoptosis is phosphatidylserine (phospholipid component in the inner leaflet of the cell membrane) moves from inner leaflet to outer leaflet of the plasma membrane when the cells undergoes apoptosis. This acts as a signal for the macrophages to engulf the cell and leads to the cell death. To quantify

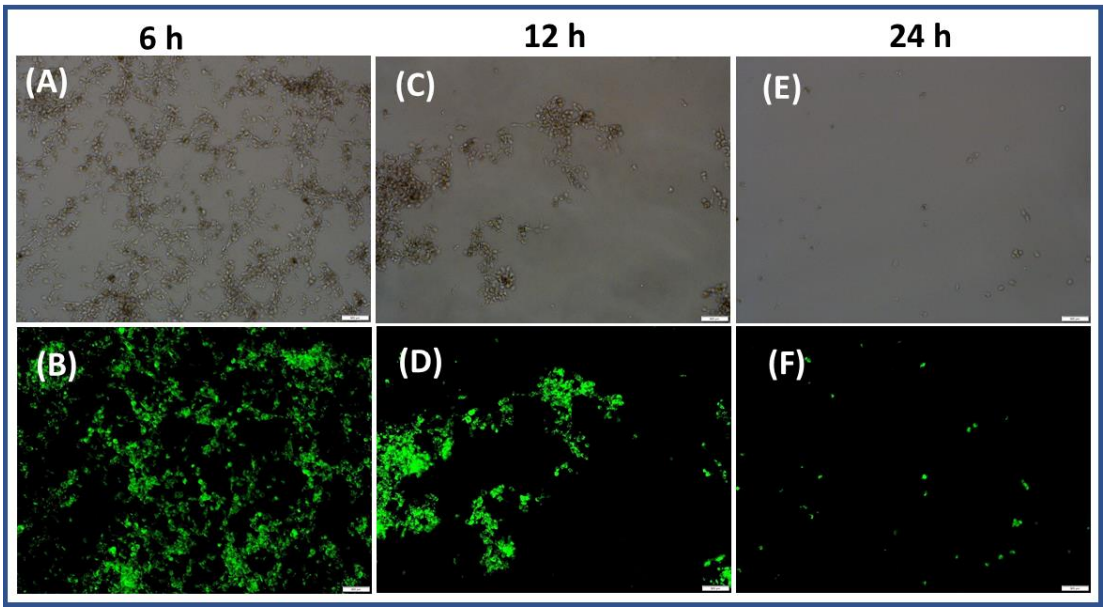

the apoptotic cell death, a protein known as Annexin-V which has higher affinity towards phosphatidylserine labelled with a fluorescent dye FITC was used. The fluorescence emitted from the cells quantifies the cell death. To perform the apoptosis, the LNCaP cells were seeded in a 12 well plate and treated with nanoparticles after attaining the 80-90% confluency. The cells were incubated with nanoparticles at different points in time: 6 h, 12 h, and 24 h, respectively. The cells were washed with PBS twice and stained with Annexin V-labelled FITC (5 µL) and Ethidium Homodimer III (5 µL) as stated in the Biotium protocol. Cells were washed twice with annexin V binding buffer and were fixed using 4% paraformaldehyde and observed under fluorescence microscope. The change in morphology of the cells was noticed as they became apoptotic and the population of the cells being reduced and getting washed away with time. The fluorescence images were obtained using Olympus IX73 Fluorescence microscope.

Figure 8: Detection of apoptotic cell death in LNCaP cells at 6 h,12 h, and 24 h in the bright field and FITC filters, respectively.

2.1.7 Comet assay: The results from all the above mentionedd studies showed there is cell death upon treating the cells with nanopraticles carrying drugs. As mentioned earlier, two of the drugs used in this project acts on DNA, to measure the extent of DNA damage possible through each of the drugs individually and as a combination therapy we performed an in vitro assay known as Comet assay. The anti-cancer drugs used in this project were known to have the synergistic potential of damaging the DNA through different mechanisms.The basic principle behind comet assay is that, head indicates undamaged DNA and tail indicates the damaged DNA where the compact structure of DNA breaks down and migrates onto the agarose gel. When the cells were treated with irinotecan, lengthy tails were formed compared with 5-fluorourcail and oxaliplatin. Upon the treatment with oxaliplatin, there was no formation of comets as it was already known in literature that oxaliplatin acts through RNA biogenesis.[106] The treatment of the cells with combination of the drugs, showed no distinct heads and all observed was the formation of tails because of the higher extent of DNA damage compared to the individual drug treatments..

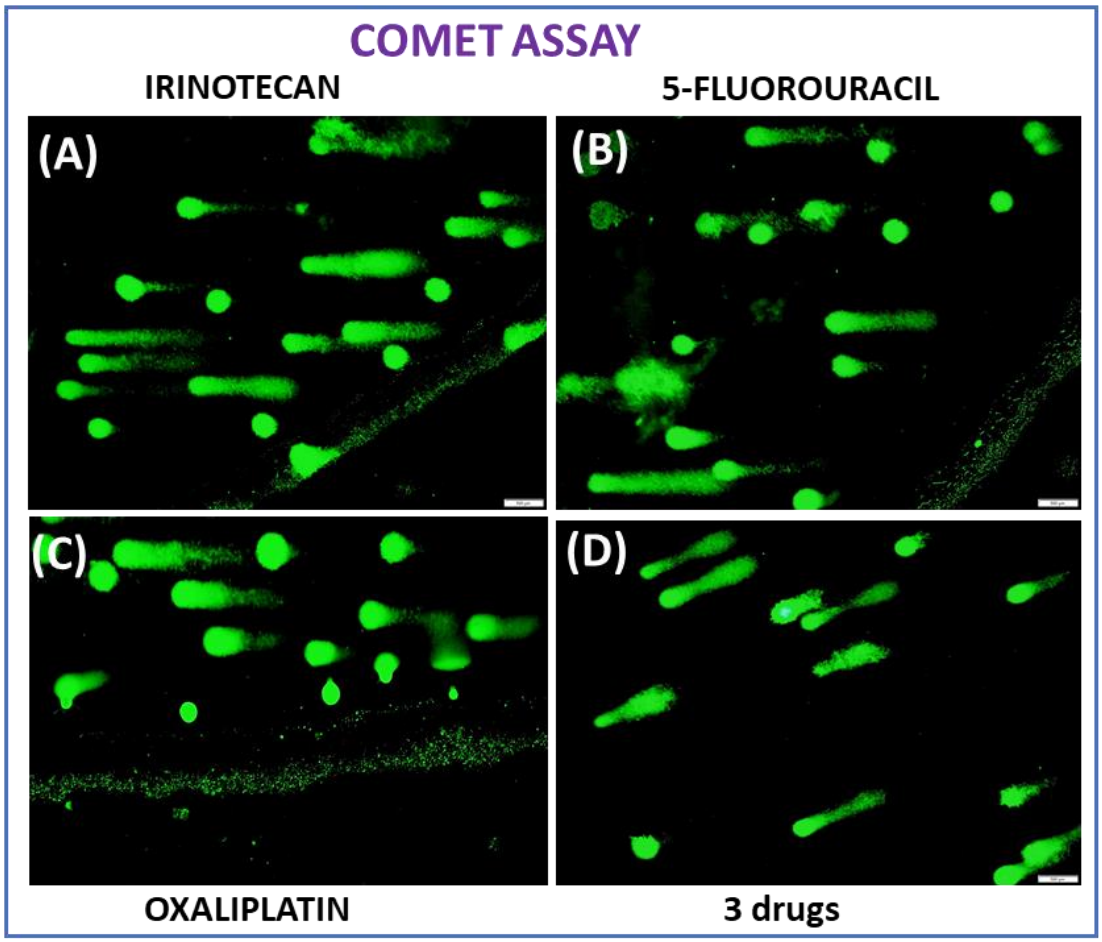

Figure 9: Determination of extent of DNA damage through comet assay. Figures (**A-D**) indicates the extent of DNA damage when treated with irinotecan, 5-Fluorouracil, oxaliplatin and three drug combination.

The DNA damage was observed visually by staining the cells with a DNA dye named SYBR gold and capturing the fluorescent images of the comet slides using an Olympus X73 fluorescence microscope. The results showed the formation of comet, indicating that cancer cell death goes through DNA damage. The % of DNA damage is directly propotional to the tail DNA and the tail moment. When the cells were treated with drugs, the extent of DNA damage was quantitatively represented in the form of tail DNA and tail moment using image J software. **Figure 10** shows the

trend in tail DNA represented in blue upon the treatment of cells with combination of drgs, ironotecan, 5-FU and oxaliplatin. Tail moment in green shows irinotecan formed lengthy tails compared to 5-FU and oxaliplatin.

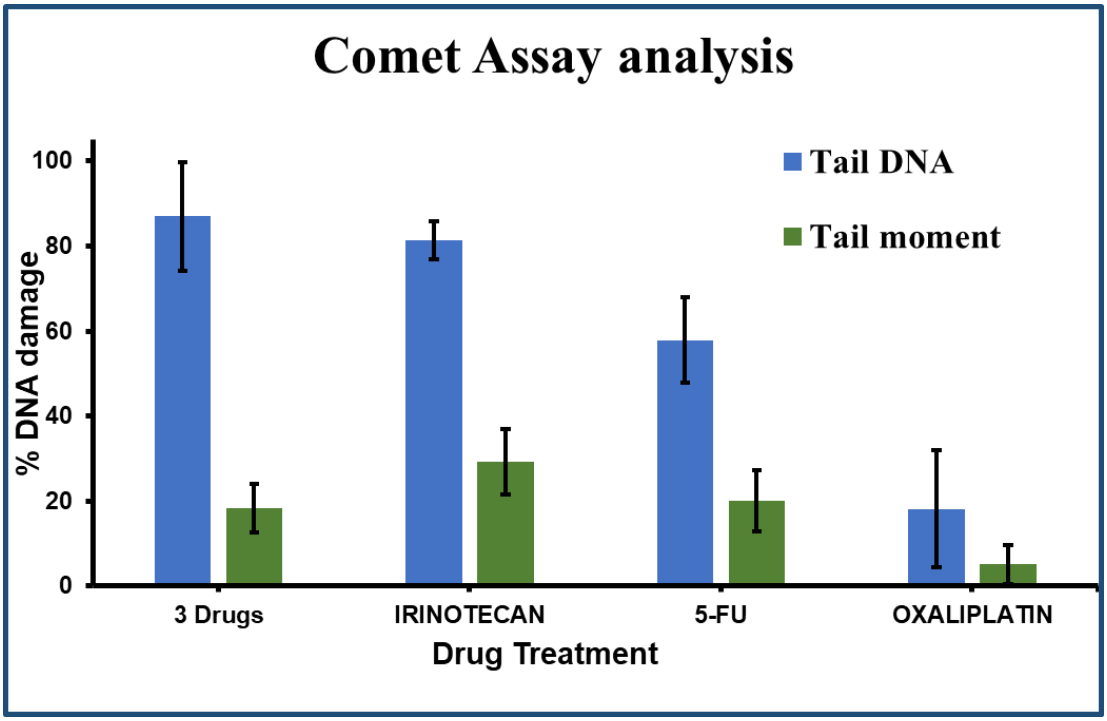

Figure 10: Tail DNA in blue and the tail moment in green indicates the extent of DNA damage on different drug treatments, irinotecan, 5-FU, oxaliplatin and combination of drugs.

2.1.8 Migration assay: As we know that prostate cancer is highly metastatic, an in vitro cell based known as migration assay/invasion assay was performed to determine the anti-metastatic potential of the anti-cancer drugs. The migration assay kit used in this assay contains two chambers, upper invasion chamber and lower feeder tray. The invasion chamber is coated with collagen through which the cells migrates from invasion chamber to feeder tray. This kit mimics the metastases process which happens in the body. The cells were treated with different drugs and incubated at 37 ℃ in presence of 5 % CO_2. Upon incubation with drugs, the migratory cells move from invasion chamber into the into the feeder tray through the collagen layer. The migratory cells were stained with a fluorescent dye named CyUQANT. The anti-metastatic potential of the drugs

was determined through the fluorescence intensity measured using Tecan i-control plate reader. The results proved that after incubation with drug(s), migration capability of the cells tremendously reduced, as lesser fluorescence emission was collected from the feeder tray in the experiment. Taken together, the three anti-cancer drugs we used were highly anti-metastatic.

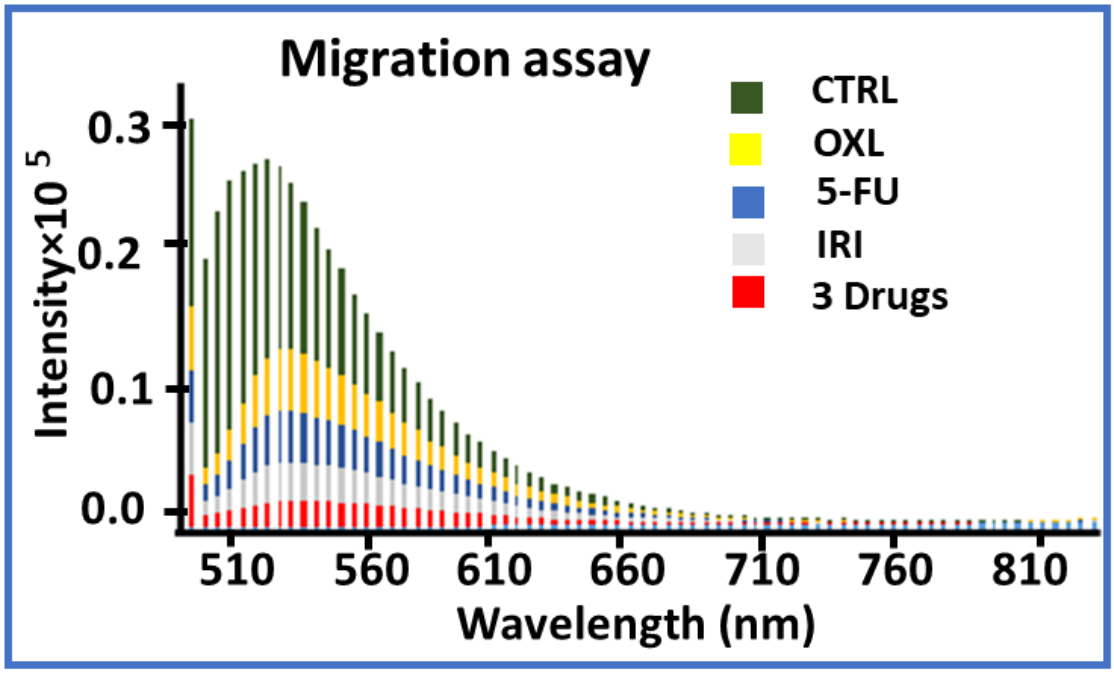

Figure 11: Determination of anti-metastatic potential using migration assay. Control cells in green showed the maximum invasion, whereas the cells treated with IONPs carrying combination of drugs in red, showed minimal invasion. The IONPs carrying individual drugs in yellow, blue, and grey showed more invasion compared to the combination treatment.

2.2 EXPERIMENTAL SECTION:

2.2.1 Materials: Iron salts (ferric chloride hexahydrate, ferrous chloride tetrahydrate), hydrochloric acid and ammonium hydroxide, Phosphate buffer saline (PBS) were ordered from Fischer Scientific. Polyacrylic acid (PAA), propargyl amine (PA), dimethylsulfoxide (DMSO), 3-(4, 5-dimethylthiazol-2-yl) - 2, 5-diphenyltetrazolium bromide (MTT), N-hydroxysuccinimide (NHS) were attained from Sigma-Aldrich. Near infrared dye (DiI-D282), and 4, 6-diamidino-2-phenylindole (DAPI-D1306) were ordered from Invitrogen. [1-ethyl-3- [3- (dimethyl amino) propyl] carbodiimide hydrochloride] (EDC) was obtained from Pierce Biotechnology. MES sodium salt was purchased from Acros Organics. The three anti-cancer drugs irinotecan, 5-Fluorouracil, oxaliplatin were acquired from Sigma Life Sciences. Dihydroethidium (DHE) was bought from Cayman Laboratories. Apoptosis and necrosis quantification kit was purchased from Biotium. SYBR gold nucleic acid gel stain was ordered from Fischer Scientific. Paraformaldehyde was purchased from Electron Microscopic Sciences. The human prostate cancer cell line LNCaP and (PC3) were obtained from ATCC. RPMI-1640 medium and Kaighn's modification of Ham's F12K medium were purchased from Corning Life Sciences. Comet assay kit, Lysis solution and LM agarose were acquired from Trevigen. Migration assay kit was purchased from Millipore.

2.2.2 Instrumentations: Using Malvern Zetasizer Nano ZS90, the average size and zeta potential of nanoparticles were measured. A Tecan Infinite M200PRO plate reader was used to study UV/Vis measurements, the absorbance of MTT, and the fluorescence of Migration assay. An Olympus IX73 Fluorescence microscope was used to capture the images of cellular uptake studies, ROS, apoptotic studies and Comet assay.

2.2.3 Synthesis of PAA coated IONPs (1): Iron oxide nanoparticles (IONPs) coated with PAA were synthesized using "water-based precipitation method". To synthesize PAA coated IONPs, three solutions were prepared. i) Iron salts solution (0.7 g of $FeCl_3$.6 H_2O and 0.4 g of $FeCl_2$ .4H_2O in 100 µL of 12 N HCl and 2 mL of DI H_2O), ii) an alkaline solution (1.8 mL of 30% NH_4OH solution in 15 mL of deionized water) and iii) stabilizing agent solution (2 g of PAA in 5 mL of DI water). The synthetic procedure was as follows: The solution of iron salts was added into alkaline solution. Afterwards, stabilizing agent (PAA in DI water) was added, and the reaction was continued

at a speed of 4000 rpm. Then, the resulting IONPs were centrifuged at 3000 rpm, 4000 rpm and 4000 rpm for 20 min each, respectively. The supernatant obtained after the final centrifugation was dialyzed in a dialysis bag has a molecular weight cut off range of 6-8 kDa. The dialysis process was done in beaker with DI water and a magnetic stirrer. The water was changed periodically for 24 h and the dialyzed IONPs were taken out of dialysis, labelled, and stored.

2.2.4 Encapsulation of DiI dye into IONPs (2): Using the solvent diffusion method, 2µL of 5 µM DiI dye, 5 µL of 2 mM irinotecan, 5 µL of 2 mM 5-fluorouracil and 5 µL of 2 mM oxaliplatin were encapsulated into 2 mL of PAA coated IONPs dropwise at a vortexing speed of 2000 rpm at intervals of time without formation of any precipitate. The drugs and dye encapsulated IONPs were set aside on table mixer at room temperature for 2 h of incubation and then dialyzed to get rid of the unreacted drugs and dye molecule. The dialyzed IONPS carrying cargos were stored at room temperature.

2.2.5 Synthesis of Propargylated IONPs (3a): Water soluble Carbodiimide chemistry (CDI) was used to prepare Propargylated IONPs and the synthetic protocol we used was as follows: i) 30 mg of EDC [1-ethyl-3-(3- dimethylaminopropyl) carbodiimide hydrochloride] in 250 µL of MES buffer (pH 6.0), ii) 22 mg of NHS [2-(N-morpholino) ethane sulfonic acid] in 250 µL of MES buffer (pH 6.0) and iii) 5 mg of propargyl amine in 500 µL of DMSO were weighed. 5 mL of IONPs were taken and the EDC

in MES buffer was added directly and mixed, NHS in MES buffer was added in 4 parts with proper mixing, and the resulting solution was kept on table mixer for 3 min of incubation. Propargyl amine in DMSO was added dropwise with proper mixing and without any precipitation. The resulting propargylated nanoparticles were kept on table mixer overnight and dialyzed against DI water for 2 h to get rid of the unreacted materials.

2.2.6 Synthesis of azide functionalized folic acid (3b): For this synthesis, i) 22 mg EDC [1-ethyl-3-(3- dimethylaminopropyl) carbodiimide hydrochloride] in 250 µL MES buffer (pH 6.0), ii) 13 mg NHS [2-(N-morpholino) ethane sulfonic acid] in 250 µL MES buffer (pH 6.0) and iii) 2.5 mg of amino propyl azide in a mixture of 200 µL DI water and 200 µL DMSO were weighed. 10 mg of folic acid was dissolved in 5 mL of 1X PBS and added EDC in MES buffer directly with proper

mixing. NHS in MES buffer was added in 4 parts with good mixing and the resulting solution was incubated for 3 min on table mixer. Amino propyl azide in the mixture of DI water and DMSO was added dropwise without any precipitation. The resulting solution was kept on the table mixer overnight.

2.2.7 Synthesis of folate conjugated IONPs (4): Folate conjugated IONPs were synthesized by adding 1.5 mL azide functionalized folic acid to 4 mL of propargylated IONPs. To the above liquid mixture, 50 µL of CuI was added from a solution of 1 mg CuI dissolved in 250 µL of DMSO. The folate conjugated IONPs were kept on table mixer overnight and dialyzed against DI water for 2 h. After the dialysis, the UV-Vis studies were performed. The presence of absorption and fluorescence peaks at 360 nm and 455 nm, respectively, which indicated the folate ligands were successfully conjugated on the surface of IONPs **(Figure 3A & 3B)**.

2.2.8 Synthesis of drugs, dye-encapsulating functional IONPs: After the successful conjugation of folate ligands on the IONPs surface, our therapeutic drugs and fluorescent dye were encapsulated into the IONP-FOL using solvent diffusion method. 2 mL of IONP-FOL was taken and encapsulated with 2 µL of 5 µM DiI dye **(2, Scheme 1),** 5 µL of 2 mM irinotecan, 5 µL of 2 mM 5-Fluorouracil and 5 µL of 2 mM oxaliplatin using Solvent diffusion method **(5, Scheme 1).** The drugs and the optical dye were dissolved in DMSO and added dropwise at a speed of 1500 rpm on a vortex mixer. The encapsulated nanoparticles were incubated on table mixer for 2 h, purified by dialysis for 2 h. The successful encapsulation of the drugs and dye was confirmed by performing the UV-Vis studies.

2.2.9 Cytotoxicity study (MTT assay): The Human prostate cancer cells (LNCaP) and (PC3) were purchased from ATCC. Both the cell lines (LNCaP and PC3) were grown in 89% RPMI 1640 and Kaighn's modification of Ham's F12K medium purchased from Corning Life Sciences. Both the media were prepared by mixing 89% media with 10% fetal bovine serum (Corning Life Sciences), and 1% Penicillin-Streptomycin antibiotic solution (10000 I.U/mL Penicillin and 10000 µg/mL Streptomycin)**.** The cells were cultured in an incubator at 37 ^{o}C with 5% CO_2. When the cells were confluent, they were seeded in 96-well plate (2500 cells /well) on the day before the experiment and incubated for 24 h. On the next day, cells were incubated with drug encapsulated

IONPs for 24 h at 37 ^{o}C. The cells were treated with nanoparticles carrying individual drugs and in combination. After that, cells were washed twice with 1X PBS and added 30 µL MTT (5 mg/mL) solution to each well and incubated at 37 ^{o}C for 4-6 h. Depending on the %cell viability, Formazan crystals were formed within this 4-6 h. The formazan crystals formed were dissolved in acidic solution (10 mL isopropanol + 250 µL 12 N HCl). The absorbance was read at a wavelength of 570 nm using an infinite M200 PRO microplate reader. Very promising results were observed. There was about 85% of cell death in LNCaP cells **(Figure 4A)** within 24 h and very less cytotoxicity was seen in the PC3 cells **(Figure 4B)**. It was proved that the targeted drug delivery was achieved through our nanoformulation.

2.3.0 Cellular uptake studies by fluorescence microscopy: Olympus IX73 fluorescence microscope was used to observe the cellular uptake using fluorescence imaging. Both the cell lines, LNCaP and PC3 were seeded in petri dishes on the previous day of the experiment. The cells were checked under the microscope for the confluency. When the cells were confluent, they were treated with specific functional nanoparticles for internalization, non-internalization, cell death studies and incubated at 37 ^{o}C for 24 h. Then, the cells were washed with 1X PBS twice and fixed with 4% formaldehyde for 10 min. The cell nuclei were stained with DAPI dye for 15 min away from the light. The non-internalization **(Figures 5A-5D)**, internalization **(Figures 5E-5H)** and cell death **(Figures 5I-5L)** in LNCaP and non-internalization in PC3 cells **(Figures 5M-5P)** were seen by capturing the images of the dishes in bright field, blue filter, red filter and merged images.

2.3.1 Assessing the levels of ROS generation in LNCaP cells: To study the measure of reactive oxidative species generation in LNCaP cells, the LNCaP cells were seeded in a 12 well plate and incubated for 24 h. After the cells were 80-90% confluent, the nanoparticles and incubated for different time points at 6 h, 12 h, 24 h, respectively, and the cells were washed with 1X PBS. The fluorescent dye DHE (300 µL of 32 mM) dye purchased from Cayman laboratories was added to the cells. The 12 well plate was kept in hood for 30 min and washed twice with 1X PBS after staining. Then 4% paraformaldehyde was added for fixation and placed in hood for 10 min. The cells were washed and covered with 1X PBS. Then the images in bright field and red filter were captured using fluorescence microscope **(Figure 6)**.

2.3.2 Quantification of apoptotic cell death in LNCaP cells: The cell death was quantified by the apoptosis and necrosis quantification kit obtained from Biotium. On the previous day of experiment, LNCaP cells were seeded in a 12 well plate. After attaining 80-90% confluency, the cells were incubated with nanoparticles at different time points: 6 h, 12 h and 24 h at 37^{o}C incubator with 5% CO_2. The cells were washed with PBS twice and stained with Annexin V-FITC (5 µL) and Ethidium Homodimer III (5 µL) as stated in the Biotium protocol. Cells were washed twice with annexin V binding buffer and were fixed using 4% paraformaldehyde. Finally, the cells were washed with annexin V binding buffer twice. The images in bright field and green filter at different time points 6 h, 12 h and 24 h were captured using Olympus IX73 fluorescence microscope **(Figure 7)**.

2.3.3 Measure of DNA damage (Comet assay): The mixture of 50 µL LNCaP cells (1×10^5/ml) and 500 µL of molten LM agarose was taken. From this, 100 µL was placed on each well of the pretreated comet slides. The slides were placed at in dark for 30 min. The slides were then immersed in lysis solution purchased from Trevigen, overnight at 4 ℃ and the excess buffer was drained out from the slides. The slides were now placed in freshly prepared alkaline unwinding solution (pH>13), followed by alkaline electrophoresis by placing slide tray adjacent to black cathode at 21 Volts for 30 min. The excess electrophoresis solution was taken out from the slides and the slides were immersed gently twice in deionized water for 5 min each and then in 70% ethanol for 5 min. The slides were placed on thermo mixer at 37 ℃ for 10-15 min and stained with 100 µL of diluted SYBR gold onto each well. Then the slides were taken from thermo mixer and rinsed in deionized water to get rid of excess dye; the slides were dried and fluorescent images were captured using IX73 Olympus fluorescence microscope.

2.3.4 Detection of anti-metastatic potential (Migration assay): The mixture of 6 mL 0.5% FBS (0.5 mL FBS+42.5 mL RPMI 1640 media + 2 mL ABAM) with 1/4th of the cell pellet was resuspended well and incubated for 24 h in a 70 mL flask. The next day, the cells were checked and found to be healthy. The cells were washed with 1X PBS twice and 5 mL of harvesting buffer was added. This was incubated for 5 min and 5 mL of quenching media was added to stop the action of trypsin. The entire solution was taken into a centrifuge tube and centrifuged at 1000 rpm

for 6 min. The quenching media was then added to the cell pellet and resuspended well. From this suspension, 100 µL was added to 30 µL of nanoparticles. The invasion chamber of the migration assay kit was rehydrated with 100 µL of 0% FBS media. After the rehydration time, 75 µL of the media was taken out of each well without touching the collagen layer. In the feeder tray, 150 µL of 10% FBS was added and the 100 µL of the samples (cell suspension with nanoparticles) were added in the invasion chamber and incubated for 24 h. On the next day, 150 µL of cell detachment buffer was added in each well of the invasion chamber with samples. The samples were taken out of the invasion chamber and placed in the wells of a 96 well plate and incubated for 30 min at 37 ℃. The feeder tray was taken out and cleaned the wells with DI water. After 30 min of incubation, 50 µL of lysis buffer and dye solution (1:75 ratio of dye and Lysis solution) was added and kept in hood for 15 min away from light. Then, 100 µL of the sample was transferred to a new well of the 96 well plate and measured the fluorescence intensity at a wavelength of 480/520 nm using Tecan-i control plate reader.

CHAPTER III

CONCLUSION AND FUTURE DIRECTION

In conclusion, it is known that prostate cancer is highly metastatic and the conventional treatment routes were not effective in showing the positive results. Because nanotechnology-based drug delivery systems have been very successful in cancer therapy, nanoformulations were designed, which has the capability of both targeting and treating prostate cancer. There were several reasons for the failure of numerous treatment options, including toxicity of drugs to the non-cancerous cells, multi-drug resistance etc. The use of the nanotechnology-based drug delivery systems in cancer therapies has been very efficacious due to their small hydrodynamic diameter (10-100 nm), which facilitates the targeted drug delivery and many other biomedical applications possible. Altogether**,** drug delivery through nanoformulation keeps the drug safe from degradation outside the target site.

In this study, we have formulated new nanotheranostic drug delivery system in the targeted treatment only to prostate cancer cells to enhance the effectiveness of conventional anti-cancer agents and to improve their toxic effects. We have synthesized iron oxide nanoparticles coated with PAA using water-based precipitation method. The surface of synthesized IONPs was decorated with folic acid (targeting ligand for folate receptor) and the anti-cancer drugs and optical dye were encapsulated via solvent diffusion method. The resulting drugs and dye carrying nanoparticles were purified using dialysis and characterized. The three drugs irinotecan, oxaliplatin, 5-Fluorouracil were used in this study to assess the therapeutic potential of their combination.

Different cell-based assays were performed. The prostate cancer cell line (LNCaP) was treated with this nanoparticle and the % cell viability was observed through MTT assay. The results showed about 85% of cell death within 24 h upon treatment of nanoparticle carrying three drug combination. Minimal toxicity was observed on the PC3 cell line when treated with nanoparticles

carrying drugs. This result specified that the functionalized nanoparticle was successful in accomplishing targeted drug delivery. The results from cellular uptake studies showed the nanoparticles achieved targeted drug delivery minimizing the toxic effects to the healthy cells. Also, the results from ROS and apoptosis showed that the nanoparticle system with anti-cancer drugs was capable of enhancing the oxidative stress in the cancer cells and causing cell death. The results from Comet assay showed these anti-cancer drugs have the capability of damaging DNA through different mechanisms. The migration assay results indicated these anti-cancer drugs have the anti-metastatic potential, which is crucial in treatment of prostate cancer. Taken together, the newly formulated nanomedicine would have tremendous effect in the targeted treatment of prostate cancer in clinical settings.

REFERENCES

(1) American Cancer society. *Cancer Facts & Figures* **2018.**

(2) Palanivelu, M.; Nair, P. V.; Krishnaswami, V.; Nethaji, R.; Surendrian, S.; Ganesan, B. Treatment of Prostate Cancer Using Nanotechnological Approaches- A Review. *International Journal of Pharmacy and Pharmaceutical Research* **2016**, 6 (2), 305-313.

(3) Sechi, G.; Eperen, V. L.; Marincola F. M.; Bianco, A.; Delogu, L. G.; Politiche, S.; Comunicazione, S.; Informazione, I. The perception of nanotechnology and nanomedicine: a worldwide social media study. *Nanomedicine* **2014**, 9, 1475-1486.

(4) Sun, C.; Jerry S.H. Lee, Zhang, M. Magnetic nanoparticles in MR imaging and drug delivery. *Advanced Drug Delivery Reviews* **2008**, 60, 1252-1265.

(5) Corot, C.; Robert, P.; Idee, J. M.; Port, M. Recent advances in iron oxide nanocrystal technology for medical imaging. *Advanced Drug Delivery Reviews* **2006**, 58, 1471-1501.

(6) Pankhurst, Q. A.; Connolly, .; Jones, S. K.; Dobson. J. Applications of magnetic nanoparticles in biomedicine, *Journal of Physics*. D, *Applied Physics* **2003**,36, R167-R181.

(7) Dobson, J. Magnetic nanoparticles for drug delivery, *Drug Development Research* **2006**, 67, 55 -60.

(8) Ito. A.; Shinkai. M.; Honda. H.; Kobayashi. T. Medical application of functionalized magnetic nanoparticles. *J.* Biosci*, Bioeng.* **2005**, 100(1): 1-11.

(9) Gupta. A. K.; Naregalkar .R. R.; Vaidya. V. D.; Gupta. M. Recent advances on surface engineering of magnetic iron oxide nanoparticles and their biomedical applications, *Nanomedicine* **2007**, 2(1), 23-29.

(10) McCarthy. J. R.; Kelly. K. A.; Sun. E. Y.; Weissleder. R. Targeted delivery of multifunctional magnetic nanoparticles. *Nanomedicine* **2007**, 2(2), 153-167.

(11) Maxwell. D. M.; Bonde. J.; Hess. D. A.; Hohm. S. A.; Lahey. R.; Creer. M. H.; Worms, D. V.; Nolta. J. A. Fluorophore conjugated iron oxide nanoparticle labelling and analysis of engrafting human hematopoietic stem cells. *Stem cells* **2008**, 26(2), 517-524.

(12) Tucker. B. A.; Rahimtula. M.; Mearow. K. M. A procedure for selecting and culturing subpopulations of neurons from rat dorsal root ganglia using magnetic beads, *Brain Res. Brain Res. Protoc* **2005**, 16(3), 50-57.

(13) Nam. J. M.; Thaxton. C. A.; Mirkin. Nanoparticle based bio-bar codes for the ultrasensitive detection of proteins. *Science* **2003**, 301 (5641), 1884-1886.

(14) Weber. C.; Falkenhagen. D. Specific blood purification by means of antibody conjugated magnetic microspheres. Scientific and clinical applications of magnetic carriers. **1997**, 371-378.

(15) Khalil, M. I. Co-precipitation in aqueous solution synthesis of magnetite nanoparticles using iron (III) salts as precursors. *Arabian Journal of Chemistry* **2015**, 8, 279-284.

(16) Unni, M.; Uhl, A. M.; Savliwala, S.; Savitzky, B. H.; Dhavalikar, R.; Garraud, N.; Arnold, D. P.; Kourkoutis, L. F.; Andrew, J. S.; Rinaldi, C. Thermal decomposition synthesis of magnetic nanoparticles with diminished magnetic dead layer by controlled addition of oxygen. *ACS Nano* **2017**, 11(2), 2284-2303.

(17) Sun, X.; Zheng, Ch.; Zhang, F.; Yang, Y.; Wu, G.; Yu, A.; Guan, N. Size controlled synthesis of magnetite (Fe3O4) nanoparticles coated with glucose and gluconic acid from a single Fe(III) precursor by bifunctional hydrothermal method. *J. Phys. Chem C* **2009**, 113,36, 16002-16009.

(18) Santra, S.; Tapec, R.; Theodoropoulou, N.; Dobson, J.; Hebard, A.; Tan, W. Synthesis, and characterization of silica coated iron oxide nanoparticles in microemulsion method: The effect of non-ionic surfactants. *Langmuir* **2001**, 17(10), 2900-2906.

(19) Kim, E. H.; Lee, H. S.; Kwak, B. K.; Kim, B. K. Synthesis of ferrofluid with magnetic nanoparticles by Sonochemical method for MRI contrast agents. *Journal of Magnetism and Magnetic Materials* **2005**, 289, 328-330.

(20) Hu, H.; Yang, H.; Haung, P.; Cui, D.; Peng, Y.; Zhang, J.; Lu, F.; Lian, J.; Shi, D. Unique role of ionic liquid in microwave assisted synthesis of monodisperse magnetite nanoparticles. *Chem. Commun*, **2010**, 46, 3866-3868.

(21) Kandasamy. G.; Maity. D. Recent advances in superparamagnetic iron oxide nanoparticles (SPIONS) for in vitro and in vivo cancer nanotheranostics. *International journal of Pharmaceutics* **2015** *,* 496, 191-218.

(22) Elfick, A. P.; Green, S. M.; McCaskie, A. W.; Birch, M. A. Opsonization of Polyethylene wear particles regulates macrophage and osteoblast responses in vitro. *J. Biomed Mater Res B Appl Biomater* **2004**, 71, 244-251.

(23) Qiao, T.; Wu, Y. H.; Jin, J.; Gao. W.; Xie, Q. Z.; Wang, S.; Zhang, Y.; Deng, H. Conjugation of catecholamines on magnetic nanoparticles coated with sulfonated chitosan. *Colloids Surf A* **2011**, 380, 169-174.

(24) Zhou, Y. T.; Nie, H. L.; Branford White C, He, Z. Y.; Zhu, L. M. Removal of Cu^{+2} from aqueous solution by chitosan-coated magnetic nanoparticles modified with alpha-ketoglutaric acid. *J. Colloid interface Sci* **2009**, 330, 29-37.

(25) Chen, H. Z.; Zhang, Z. H.; Luo, L. J.; Yao, S. Z. Surface imprinted chitosan coated magnetic nanoparticles modified multi walled carbon nanotubes biosensor detection of bovine serum albumin. *Sensors Actuators B Chem* **2012** , 163, 76-83.

(26) Kim, D. H.; Kim, K. N.; Kim, K. M.; Lee, Y. K. Targeting to carcinoma cells with chitosan and starch coated nanoparticles for magnetic hyperthermia. *J. Biomed Mater Res A* **2009** , 88A,1-11.

(27) Kurowia, T.; Noguchi, Y.; Nakajima, M.; Sato, S.; Mukataka, S.; Ichikawa, S. Production of chitosan oligosaccharides using chitosanase immobilized on amylose-coated magnetic nanoparticles. *Process Biochem* **2008**,43, 62-9.

(28) Li, G. Y.; Zhou, Z. D.; Li, Y. J.; Haung, K. I.; Zhong, M. Surface functionalization of chitosan-coated magnetic nanoparticles for covalent immobilization of yeast alcohol dehydrogenase from Saccharomyces cerevisiae. *J Magn Magn Mater,* **2010**, 322, 3862-8.

(29) Peng, Q. Q.; Liu, Y. J.; Zeng, G. M.; Xu, W. H.; Yang, C. P.; Zhang, J. J.; Biosorption of copper (ii) by immobilizing Saccharomyces cerevisiae on the surface of chitosan-coated magnetic nanoparticles from aqueous solution. *J. Hazard Mater*, **2010**,177, 676-82.

(30) Hong, S.; Chang, Y.; Rhee, I. Chitosan-coated ferrite nanoparticles as T-2 contrast agent for magnetic resonance imaging. *J. Korean Phys Soc*, **2010**, 56, 868-73.

(31) Chawla, K.; Lee, S.; Lee, B. P.; Dalsin, J. L.; Messersmith, P. B.; Spencer, N. D.; A novel low friction surface for bio medical applications: modification of poly(dimethylsiloxane) PDMS with poly ethylene glycol (PEG)-DOPA-lysine. *J. Biomed Mater Res*, **2009**, 90, 742-9.

(32) Chu, C. H.; Wang, Y. C.; Haung, H. Y.; Wu, L. C.; Yang, C. S.; Ultrafine PEG-coated polylactic-co-glycolic acid) nanoparticles formulated by hydrophobic surfactant-assisted-one-pot synthesis for biomedical applications. *Nanotechnology*, **2011**, 22, 185601.

(33) Inada, Y.; Furukawa, M.; Sasaki, H.; Kodera, Y.; Hiroto, M.; Nishimura, H.; Matsushima, A. Biomedical and biotechnological applications of PEG- and PM-modified proteins. *Trends Biotechnol* **1995**, 13, 86-91.

(34) Park, J. Y.; Daksha, P.; Lee, G. H.; Woo, S.; Chang, Y. Highly water-dispersible PEG surface modified ultra-superparamagnetic ironoxide nanoparticles useful for target specific biomedical applications. *Nanotechnology*, **2008**, 19, 365603.

(35) Betancourt, T.; Byrne, J. D.; Sunaryo, N.; Crowder, S. W.; Kadapakkam, M.; Patel, S.; Casciato, S.; Lisa, B-P.; Brannon-Peppas L. PEGylation strategies for active targeting of PLA/PLGA nanoparticles. *J. Biomed Mater Res A*, **2009**, 91, 263-76.

(36) Choi, K.Y.; Min, K. H.; Yoon, H. Y.; Kim, K.; Park, J. H.; Kwon, I. C.; Choi, K.; Jeong, S. Y. PEGylation of hyaluronic acid improves tumor targetability in vivo. *Biomaterials*, **2011**, 32, 1880-9.

(37) Mengersen, F.; Bunjes, H.; PEGylation of super cooled smectic cholesteryl myristate nanoparticles. *Eur J Pharm Biopharm*, **2012**, 81, 409-17.

(38) Miki, K.; Oride, K.; Inoue, S.; Kuramochi, Y.; Nayak, R. R.; Matsuoka, H.; Harada, H.; Hiraoka, M.; Ohe, K. Ring opening metatheses polymerization-based synthesis of polymeric nanoparticles for enhanced tumor imaging in vivo: Synergistic effect of Folate receptor targeting and PEGylation. *Biomaterials*, **2010**, 31, 934-42.

(39) Ozcan, I.; Segura-Sanchez F.; Bouchemal, K.; Sezak, M.; Ozer, O.; Guneri, T.; Ponchel, G. PEGylation of poly(gamma-benzyl-L-glutamate)nanoparticles is efficient for avoiding mononuclear phagocyte system capture in rats. *Int J Nanomedicine*, **2010**, 5, 1103-11.

(40) Suh, J.; Choy, K. L.; Lai, S. K.; Suk, J. S.; Tang, B. C.; Prabhu, S.; Hanes, J. PEGylation of nanoparticles improves their cytoplasmic transport. *Int J. Nanomedicine*, **2007**, 2, 735-41.

(41) Vasudev, S. S.; Ahmad, S.; Parveen, R.; Ahmad, F. J.; Anish, C. K.; Ali, M.; Panda, A. K. Formulation of PEGylated L-asparaginase loaded poly(lactide-co-glycolide) nanoparticles: Influence of pegylation on enzyme loading activity, in vitro release. *Pharmazie*, **2011**, 66, 956-60.

(42) Zhang, Y.; Chen, J.; Pan, Y.; Zhao, J.; Ren, L.; Liao, M.; Hu, Z.; Kong, L.; Wang, J. A novel PEGylation of chitosan nanoparticles for gene delivery. *Biotechnol Appl Biochem*, **2007**, 46,197-204.

(43) Yu, M.; Huang, S. H.; Yu, K. J.; Clyne, A. M.; Dextran and PEG-coating reduce both 5 nm and 30 nm iron oxide nanoparticle cytotoxicity in 2D and 3 D cell culture. *Int J Mol Sci*, **2012**, 13,5554-70.

(44) Mahmoudi, M.; Simchi, A.; Imani, M.; Milani, A. S.; Stroeve, P. Optimal design and characterization of superparamagnetic iron oxide nanoparticles coated with poly vinyl alcohol for targeted delivery and imaging. *J Phys Chem B*, **2008**, 112, 14470-81.

(45) Kayal, S.; Ramanujam, R. V.; Doxorubicin loaded PVA coated iron oxide nanoparticles for targeted drug delivery. *Mater Sci Eng C Mater*, **2010**, 30, 484-90.

(46) Zhang, Y.; Liu, J. Y.; Ma, S.; Zhang, Y. J.; Zhao, X.; Zhang, X. D. Synthesis of PVP-coated ultra-small Fe_3O_4 nanoparticles as an MRI contrast agent. *J. Mater Sci Mater Med*, **2010**, 21, 1205-10.

(47) Burugupalli, K.; Koul, V.; Dinda, A. K. Effect of composition of interpenetrating polymer network hydrogels based on poly(acrylic acid) and gelatin on tissue response: a quantitative in vivo study. *J. Biomed Mater Res*, **2004**, 68A(2), 210-8.

(48) Makaida, H. K.; Seigel, S. J. Poly9Lactic co-glycolic acid) PLGA as biodegradable controlled drug delivery carrier. *Polymers (Basel)*, **2011**, 3(3), 1377-1397.

(49) Danhier, F.; Ansorena, E.; Silva, J. M.; Coco, R.; Breton, A. L.; Preat, V. PLGA-based nanoparticles: An overview of biomedical applications. *Journal of controlled issues*, **2012**, 161(2), 505-522.

(50) Muller, J. P.; Gahde, J.; Mehner, H.; Menzel, M.; Guttler, B. Plasma assisted transformation of iron surfaces into magnetite. *Surface and coatings technology*, **1999**, 116-119, 367-369.

(51) Qian, Z. M.; Li, H.; Sun, H.; Ho, K. Targeted delivery via transferrin receptor-mediated endocytosis pathway. *Pharmacol Rev*, **2002**, 54(4), 561-87.

(52) Moore, A.; Basilion, J.; Chiocca, E. A.; Weissleder, R. Measuring Transferrin receptor gene expression by NMR imaging. *Biochem Biophys Acta*, **1998**, 1402, 239-49.

(53) Berry, C. C.; Charles, S.; Wells, S.; Dalby, M. J.; Curtis, A. S. G. The influence of transferrin stabilized magnetic nanoparticles on human dermal fibroblasts in culture. *Int J Pharm*, **2004**, 269(1), 211-25.

(54) Moore, A.; Josephon, L.; Bhorade, R. M.; Basilion, J. P.; Weissleder, R. Human transferrin receptor gene as a marker gene for MR imaging. *Radiology*, **2001**, 221, 224-50.

(55) Josephson, L.; Tung, C-H.; Moore, A.; Weissleder, R. High efficiency intracellular magnetic labeling with novel superparamagnetic Tat-peptide conjugates, *Bioconj Chem*, **1999**, 10(2), 1886-91.

(56) Lewin, M.; Carlesso, N.; Tung, C-H.; Tang, X-W.; Cory, D.; Scadden, T.; Weissleder, R. Tat peptide-derivatized magnetic nanoparticles allow in vivo tracking and recovery of progenitor cells. *Nat Biotechnol*, **2000**, 18, 410-4.

(57) Zhang, Y.; Kohler, N.; Zhang, M. Surface modification of superparamagnetic magnetite nanoparticles and their intracellular uptake. *Biomaterials*, **2002**, 23(7), 1553-61.

(58) Rodney,S.; Shah, T. T.; Patel, H. R. H.; Arya, M. Key papers in prostate cancer. *Expert Rev. Anticancer Ther*, **2014**, 1-6.

(59) Jain, S.; Hirst, D. G.; Sullivan, J. M. O. Gold nanoparticles as novel agents for cancer therapy. *Br J. Radiol*, **2012**, 85 (1010) , 101-113.

(60) Prabhu, R. H.; Patravale, V. B.; Joshi, M. D. Polymeric nanoparticles for targeted treatment in oncology: current insights, *Int J. Nanomedicine*, **2015**, 10, 1001-1018.

(61) Caputo, F.; Mameli, M.; Sienkiewicz, A.; Licoccia, S.; Stellacci, F.; Ghibelli, L.; Traversa, E. A novel synthetic approach of cerium oxide nanoparticles with improved biomedical activity. *Scientific reports*, **2017**, 7, 4636.

(62) Revia, R. A.; Zhang, M. Magnetite nanoparticles for cancer diagnosis, treatment, and treatment monitoring. *Materials today*, **2016**, 19 (3), 157-168.

(63) Fanq, M.; Chen, M.; Liu, L.; Li, Y. Application of quantum dots in detection and diagnosis of cancer: A review. *J. Biomedical nanotechnology*, **2017**, 13(1), 1-16.

(64) Chen, Z.; Zhang, A.; Wang, X.; Zhu, J.; Fan, Y.; Hu, Y.; Yang, Z. The advances of carbon nanotubes in cancer diagnostics and therapeutics. *Journal of nanomaterials*, **2017**.

(65) Grothey, A.; Sargent, D.; Goldberg, R. M.; Schmoll, H. J. Survival of patients with advanced colorectal cancer improved with availability of Fluorouracil, Leucovorin, Oxaliplatin, Irinotecan in the course of tretament. *Clinical Oncology*, **2004**, 22, 1209-1214.

(66) Conroy, T.; Paillot, B.; Francois, E.; Bugat, R.; Jacob, J-H.; Stein, U.; Nasca, S.; Metges, J-H.; Rixe, O.; Michelle, P.;Magherini, E.; Hua, A.; Deplanque, G. Irinotecan plus Oxaliplatin and Leucovorin-Modulated fluorouracil in advanced pancreatic cancer. *J. Clin Oncol*, **2005**, 23, 1228-1236.

(67) Mans, D. R. A.; Grivicich, I.; Peters, G. J .; Schwartsmann, G. Sequence dependent growth inhibition and DNA damage formation by irinotecan-5-fluorouracil combination in human colon carcinoma cell lines. *Eur J Cancer*, **1999**, 35, 1851-1861.

(68) Raymond, E.; Christine, B-F.; Djelloul, S.; Mester J.; Cvitkovic, E.; Allain, P.; Louvet, C.; Gespach, C. Antitumor activity of oxaliplatin in combination with 5-fluorouracil and thymidylase synthase inhibitor AG337 in human colon, breast, and ovarian cancers. *Anticancer Drugs*,**1997**, 8, 876-885.

(69) Nadia, Z-S.; Raymond, E.; Cvitkovic, E.; Goldwasser, F. Cellular pharmacology of combination of the DNA topoisomerase I inhibitor SN 38 and the diaminocyclohexane platinum derivative oxaliplatin. *Clin Cancer Res*, **1999**, 5, 1189-1196.

(70) Raymond, E.; Faivre, S.; Chaney, S. Woynarowski, J.; Cvitkovic, E. Cellular and molecular pharmacology of oxaliplatin. *Mol Cancer Ther*, **2002**, 1, 227-235.

(71) Sorbero, A. F. Scheduling of fluorouracil: a forget-me-not in the jungle of doublets. *J. Clin Oncol*, **2004**, 22, 4-6.

(72) Douillard, J. Y.; Cunningham, D.; Roth, A. D.; Navarro, M.D.; James, R. D.; Karasek, P.; Jandik, P.; Iveson, T.; Carmichael, J.; Alakl, M.; Gruia, G.; Awad, L.; Rougier, P. Irinotecan combined with fluorouracil compared with fluorouracil alone as first-line treatment for metastatic colorectal cancer: a multicenter randomized trial. *Lancet*, **2000**, 335, 1041-1047.

(73) Saltz, L. B.; Cox, V. J.; Blanke, C.; Rosen, L. S.; Fehrenbacher, L.; Moore, M.J.; Maroun, J. A.; Ackland, S. P.; Locker, P. K.; Pirotta, N.; Elfring, G. L.; Miller, L. L. Irinotecan plus fluorouracil and leucovorin for metastatic colorectal cancer .*N. Engl J. Med*, **2000**, 343, 9045-914.

(74) Giacchetti, S.; Perpoint, B.; Zidani, R.; Faggiuolo, R.; Focan, C.; Chollet, P.; Llory, J. F.; Letourneau, Y.; Coudert, B.; Domoinique, L. F.; Walter, S.; Adam, R.; Le Rol, A.; Misset, J. L.; Levi, F. Phase III multicenter randomized trial of oxaliplatin added to chronomodulated fluorouracil -leucovorin as first line tretament of metastatic colorectal cancer. *J. Clin Oncol,* **2000***,* 18(1), 136-47.

(75) de Gramont, A.; Figer, A.; Seymour, M.; Homerin, M.; Hmissi, A.; Cassidy, J.; Boni, C.;Cortes-Funes, H.; Cervantes, A.; Freyer, G.; Papamichael, D.; Le Bail, N.; Louvet, C.; Hendler, D.; de Braud, F.; Wilson, C.; Morvan, F.; Bonetti, A. Leucovorin and fluorouracil with or without oxaliplatin as first-line treatment in advanced colorectal cancer, *J. Clin Oncol*, **2000**,18, 2938-2947.

(76) Masi, G.; Allergrini, G.; Cupini, S.; Marcucci, L.; Cerri, E.; Brunetti, I.; Fontana, E.; Ricci, S.; Andraceutti, S.; Falcone, A. First line tretament of metastatic colorectal cancer with irinotecan, oxaliplatin, 5fluorouracil/leucovorin (FOLFOXFIRI): Results of a phase II study with a simplified biweekly schedule. *Annals of Oncol*, **2004**,15, 1766-1772.

(77) Giacchetti, S.; Itzhaki, M.; Gruia, G.;Adam, R.; Zidani, R.; Kunstingler, F.; Brienza, S.; Berteault, C. V.; Jasmin, C.; Reynes, M.; Bismuth, H.; Misset, J. L.; Levi, F. Long term survival of patients with unresectable colorectal cancer liver metastases following infusional chemotherapy with 5-fluorouracil, leucovorin, oxaliplatin and surgery. *Ann Oncol*, **1999**, 10,6663-669.

(78) Adam, R.; Avisar, E, Ariche, A.; Giacchetti, S.; Azoulay, D.; Castaing, D.; Kunstingler, F.; Levi, F.; Bismuth, F. Five-year survival following hepatic resection after neoadjuvant therapy for nonresectable colorectal cancer. *Ann Surg Oncol*, **2001**, 8, 347-353.

(79) Tournigand, C.; Andre, T.; Achille, E.; FOLFIRI followed by FOLFOX6 or the reverse sequence in advanced colorectal cancer: A randomized GERCOR study. *J.Clin Oncol*, **2004**, 22, 229-237.

(80) Goldberg, R. M.; Sargent, D. J.; Morton, R. F.; Fuchs, C, S.; Ramanathan, R. K.; Williamson, S. K.; Findlay, B. P.; Pilot, H. C.; Alberts, S, R. A randomized controlled trial of fluorouracil plus leucovorin, irinotecan and oxaliplatin combinations in patients with previously untreated metastatic colorectal cancer. *J. Clin Oncol*, **2004**, 22, 1209-1214.

(81) Falcone, A.; Masi, G.; Allergini, G.; Biweekly chemotherapy with oxaliplatin, irinotecan, infusional fluorouracil, and leucovorin: A pilot study in patients with metastatic colorectal cancer. *J. Clin Oncol*, **2002**, 20, 4006-4014.

(82) Souglakos, J.; Mavroudis, D.; Kakolyris, S.; Kourousisi, Ch.; Vardakis, N.; Androulakis, N.; Agelaki, S.; Kalbakis, K.; Tsetis, D.; Athanasiadis, N.; Samonis, G.; Georgoulias, V. Triplet combination with irinotecan plus oxaliplatin plus continuous-infusion of fluorouracil and leucovorin as first line treatment in metastatic colorectal cancer: A multicenter phase II trial. *J. Clin Oncol*, **2002**, 20, 2651-2657.

(83) Ychou, M.; Conroy, T.; Seitz, J. F.; Gourgou, S.; Hua, A, Mery-Mignard, A.; Kramar, A. An open phase I study assessing the feasibility of the triple combination: oxaliplatin plus irinotecan plus leucovorin/5-fluorouracil every 2 weeks in patients with advanced solid tumors. *Ann Oncol*, **2002**, 14, 481-489.

(84) Calvo, E.; Cortes, J.; Rodriguez, J.; Fernandez-Hidalgo, O.; Rebollo, J.; Martin-Algarra, S.; Garcia-Foncillas, J.; Martinez-Monge, R.; de Irala, J.; Brugarolas, A. Irinotecan, oxaliplatin, and 5-fluorouracil/leucovorin combination chemotherapy in advanced colorectal carcinoma: A phase II study. *Clin Colorectal Cancer*, **2002**, 2, 104-110.

(85) Garufi, C.; Bria, E.; Vanni, B.; Zappala, A. M. R.; Sperduti, I.; Terzoli, F. A phase II study of irinotecan plus chronomodulated oxaliplatin, 5-fluorouracil and folinic acid in advanced colorectal cancer patients. *British Journal of Cancer*, **2003**, 89, 1870-1875.

(86) Comella, P.; Casaretti, R.; De Rosa, V.; Avallone, A.; Izzo, F.; Fiore, F.; Lapenta, L.; Comella, G. Oxaliplatin plus irinotecan and leucovorin-modulated 5-fluorouracil triplet regimen every other week: A dose finding study in patients with advanced gastrointestinal malignancies. *Ann Oncol*, **2002**, 13, 1874-1881.

(87) Goetz, M. P.; Erlichmann, C.; Windebank, A. J.; Reid, J.M.; Sloan, J. A.; Atheron, P.; Adeji, A. A.; Rubin, J.; Pilot, H.; Galanis, E.; Ames, M. M.; Goldberg, R. M.; Phase I and pharmacokinetic study of two different schedules of oxaliplatin, irinotecan, fluorouracil, and leucovorin in patients with solid tumors. *J. Clin Oncol*, **2003**, 21 (20), 3761-9.

(88) Fischel, J. L.; Rostango, P.; Formento, P.; Dubreuil, A.; Etienne, M-C.; Milano, G. Ternary combination of irinotecan, fluorouracil-folinic acid and oxaliplatin : Results on human colon cancer cell lines. *British Journal of Cancer*, **2001**, 84, 579-585.

(89) Bleiberg, H.; de Gramont, A.; Oxaliplatin plus 5-fluorouracil : Clinical experience in patients with advanced colorectal cancer. *Semin Oncol*, **1998**, 25, 32-39.

(90) Andre, T.; Bensamine, M. A.; Louvet, C.; Multicenter phase II study of bimonthly high-dose leucovorin, fluorouracil infusion, and oxaliplatin for metastatic colorectal cancer resistant to the same leucovorin and fluorouracil regimen. *J Clin Oncol*, **1999**, 17, 3560-3568.

(91) Levi, F, Zidani, R.; Vannetzel, J-M.; Perpoint, B.; Focan, C.; Faggiuolo, R.; Chollet, p.; Garufi, C.; Itzhaki, M.; Dogliotti, L. Chronomodulated versus fixed-infusion-rate delivery of ambulatory

chemotherapy with oxaliplatin, fluorouracil, and folinic acid (leucovorin) in patients with colorectal cancer metastases: A randomized multi-institutional trial. *J Natnl Cancer Inst*, **1994**, 86, 1608-1617.

(92) Levi, F.; Zidani, R.; Misset, L-L.; Randomized multicenter trial of chronotherapy with oxaliplatin, fluorouracil and folinic acid in metastatic colorectal cancer. *Lancet*, **1997**, 350, 681-686.

(93) Vanhoufer, U.; Haarstrick, A.; Achterrrah, W.; Cao, S.; Seeber, S.; Rustum, Y. M. Irinotecan in the treatment of colorectal cancer: A clinical overview. *J Clin Oncol*, **2001**, 19, 1501-1518.

(94) Rougier, P.; Van Custem, E; Bajetta, E.; Niederle, N.; Possinger, K.; Labianca, R.; Navarro, M.; Morant, R.; Bleiberg, H.; Wils, J.; Awad, L.; Herait, P.; Jacques, P. Randomized trial of irinotecan versus fluorouracil by continuous infusion after fluorouracil failure in patients with metastatic colorectal cancer. *Lancet*, **1998**, 352, 1407-1412.

(95) Cunningham, D.; Pyrhonen, S.; James, R. D.; Punt, C. J.; Hickish, T. F.; Hiekkila, R.; Johannesen, T. B.; Starkhammar, T.; Topham, C. A.; Awad, L.; Jacques, C.; Herait, P. Randomized trial of irinotecan plus supportive care versus supportive care aloe after fluorouracil failure for patients with metastatic colorectal cancer. Lancet, 1998, 352, 1413-1418.

(96) Comella, P.; Crucitta, E.; De Vita, F.; De Lucia, L.; Farris, A.; Del Gaizo, F.; Palmeri, S.; Lannelli, A.; Mancarella, S.; Tafuto, S.; Maiorino, L.; Buzzi, F.; De Cataldis, G. Biweekly irinotecan combined with folinic acid-modulated 5-fluorouracil i.v. bolus in advanced colorectal carcinoma.

(97) Cao, S.; Rustum, Y. M. Synergistic antitumor activity of irinotecan in combination with 5-fluorouracil in rats bearing advanced colorectal cancer: Role of drug sequence and dose. *Cancer Res*, **2000**,60, 3717-3721.

(98) Placensia, C.; Taron, M.; Abad, A.; Rosell, R.; Synergism of oxaliplatin (OXA) with either 5-fluorouracil (5FU) or topoisomerase I inhibitor in sensitive and 5FU resistant colorectal cancer cell lines is independent of DNA-mismatch repair and p53 status. *Proc Am Soc Clin Oncol*, **2000**, 19.

(99) Fischel, J-L.; Etienne, M-C.; Formento, P.; Milano, G.; Search for optimal schedule for the oxaliplatin/5-fluorouracil association modulated or not by folinic acid. Preclinical data. *Clin Cancer Res*, **1998**, 4, 2529-2535.

(100) de Gramont, A.; Vignoud, J.; Tournigand, C.; Louvet, C.; Andre, T.; Varette, C.; Raymond, E.; Moreau, S.; Le bail, N.; Krulik, M. Oxaliplatin with high-dose leucovorin and 5-fluorouracil 48-hour continuous infusion in pre-treated metastatic colorectal cancer. *Eur J Cancer*, **1997**, 33, 214-217.

(101) Maindrault-Goebel, F.; Louvet, C.; Andre, T.; Oxaliplatin added to the simplified bimonthly leucovorin and 5-fluorouracil regimen as second-line treatment for metastatic colorectal cancer. *Eur J Cancer*, **1999**, 35, 1338-1342.

(102) Maindrault-Goebel, F.; Louvet, C.; Andre, T.; High dose intensity oxaliplatin added to the to the simplified bimonthly leucovorin and 5-fluorouracil regimen as second-line treatment for metastatic colorectal cancer (FOLFOX7). *Eur J Cancer*, **2000**, 37, 1000-1005.

(103) Santra, S.; Kaittanis, C.; Grimm, J.; Perez, J. M. Drug/Dye-loaded, Multifunctional Iron Oxide Nanoparticles for Combined Targeted Cancer Therapy and Dual Optical/Magnetic Resonance Imaging. *Small*, **2009**, 5 (16), 1862-1868.

(104) Flores, O.; Santra, S.; Kaittanis, C.; Bassiouni, R.; Khaled, A-S.; Khaled, A-R.; Grimm, J.; Perez, J. M. PSMA-Targeted Theranostic Nanocarrier for Prostate Cancer. *Theranostics*, **2017**, 7(9), 2477-2494.

(105) Sulthana, S.; Banerjee, T.; Kallu, J.; Vuppala, S-R.; Heckert, B.; Naz, S.; Shelby, T.; Yambem, O.; Santra, S. Combination Therapy of NSCLC Using Hsp90 Inhibitor and Doxorubicin Carrying Functional Nanoceria. *Mol. Pharmaceutics*, **2017**, 14, 875-884.

(106) Bruno, P-M.; Liu, Y.; Park, G. Y.; Murai, J.; Koch, C-E.; Eisen, T-J.; Pritchard, J-R.; Pommier, Y.; Lippard, S-J.; Hemann, M-T. A subset of platinum containing compounds kill cells by inducing ribosome biogenesis stress rather than by engaging DNA damage response. *Nat. Med*, **2017**, 23(4), 461-471.